


RESEARCH

Open Access



# Induced pluripotent stem cell-derived mesenchymal stem cells (iMSCs) inhibit M1 macrophage polarization and reduce alveolar bone loss associated with periodontitis

Liang Chen<sup>1</sup>, Yuanqing Liu<sup>1</sup>, Chenhao Yu<sup>1</sup>, Pei Cao<sup>1</sup>, Yiming Ma<sup>1</sup>, Yiran Geng<sup>1</sup>, Yu Cai<sup>1</sup>, Yong Zhang<sup>2</sup>, Jia Liu<sup>1</sup>, Yang Li<sup>3\*</sup> and Qingxian Luan<sup>1\*</sup> 

## Abstract

**Background** Periodontitis is a chronic inflammatory disease and macrophages play a pivotal role in the progression of periodontitis. Mesenchymal stem cells (MSCs) have emerged as potential therapeutic agents for the treatment of periodontitis due to their immunomodulatory properties and capacity for tissue regeneration. Compared to conventionally derived MSCs, induced pluripotent stem cell-derived MSCs (iMSCs) offer distinct advantages as promising candidates for MSC-based therapies, owing to their non-invasive acquisition methods and virtually unlimited availability. This study aims to investigate the effects and mechanisms of iMSCs in modulating macrophage polarization and alleviating periodontitis-related alveolar bone loss.

**Methods** iMSCs were generated from iPSCs and characterized for differentiation potential. The effects of iMSCs on macrophage polarization were evaluated using THP-1-derived macrophages under inflammatory conditions (LPS and IFN- $\gamma$  stimulation). Co-culture assays, cytokine analysis, reactive oxygen species (ROS) detection, transcriptomic analysis, flow cytometry, reverse transcription-quantitative polymerase chain reaction (RT-qPCR), and western blot analysis were performed to elucidate the underlying mechanisms. The therapeutic potential of iMSCs was assessed in a ligature-induced periodontitis mouse model using micro-CT, histological analysis, and immunofluorescence staining.

**Results** iMSCs inhibit M1 macrophage polarization through the suppression of the NF- $\kappa$ B signaling pathway. Additionally, iMSCs reduce the production of pro-inflammatory cytokines (IL-1 $\beta$ , IL-17) and reactive oxygen species (ROS), while enhancing the secretion of anti-inflammatory cytokines (IL-10) and growth factors (VEGF), thereby improving the inflammatory microenvironment. Under inflammatory conditions, iMSCs preserve the osteogenic potential of periodontal ligament stem cells (PDLSCs) and alleviate alveolar bone loss in mice with periodontitis. In vivo, iMSCs reduce the number of M1 macrophages and inhibit the activation of NF- $\kappa$ B in periodontal tissues, supporting their anti-inflammatory and immunomodulatory effects.

\*Correspondence:

Yang Li

liyang@bjmu.edu.cn

Qingxian Luan

kqluanqx@bjmu.edu.cn

Full list of author information is available at the end of the article



© The Author(s) 2025. **Open Access** This article is licensed under a Creative Commons Attribution-NonCommercial-NoDerivatives 4.0 International License, which permits any non-commercial use, sharing, distribution and reproduction in any medium or format, as long as you give appropriate credit to the original author(s) and the source, provide a link to the Creative Commons licence, and indicate if you modified the licensed material. You do not have permission under this licence to share adapted material derived from this article or parts of it. The images or other third party material in this article are included in the article's Creative Commons licence, unless indicated otherwise in a credit line to the material. If material is not included in the article's Creative Commons licence and your intended use is not permitted by statutory regulation or exceeds the permitted use, you will need to obtain permission directly from the copyright holder. To view a copy of this licence, visit <http://creativecommons.org/licenses/by-nc-nd/4.0/>.

**Conclusion** iMSCs demonstrate significant therapeutic potential in periodontitis by modulating macrophage polarization, reducing oxidative stress, and mitigating alveolar bone loss associated with the disease. These findings provide new insights into the mechanisms of iMSCs and their application as cell-based therapies for periodontal diseases.

**Keywords** Induced pluripotent stem cells, Mesenchymal stem cells, Macrophage polarization, Periodontitis, NF- $\kappa$ B signaling pathway, Alveolar bone loss, Cytokines, Oxidative stress, Periodontal ligament stem cells

## Background

Periodontitis is a chronic and progressive inflammatory disease triggered by bacterial biofilms, characterized by the sustained destruction of periodontal tissues, ultimately leading to alveolar bone loss and tooth exfoliation [1]. The pathogenesis of periodontitis involves complex immune and inflammatory responses. When pathogenic microorganisms invade the gingival tissues, the host immune system initiates a series of inflammatory reactions to combat the infection. However, excessive or prolonged activation of these responses may result in self-inflicted tissue damage, causing irreversible destruction of periodontal tissues [2].

As key immune cells in the early inflammatory response of periodontitis, macrophages play a dual role in periodontal tissues, both eliminating pathogens and potentially inducing localized inflammatory damage, thereby contributing significantly to the progression of inflammation [3, 4]. Macrophages can differentiate into distinct functional phenotypes, including pro-inflammatory M1 macrophages and anti-inflammatory M2 macrophages [5]. In infected tissues, macrophages initially polarize toward the M1 phenotype to aid in pathogen clearance. Subsequently, macrophages undergo polarization to the M2 phenotype to mediate anti-inflammatory responses and facilitate tissue repair [5]. During the pathogenesis of periodontitis, M1 macrophages are activated to produce large quantities of pro-inflammatory cytokines, such as TNF- $\alpha$  and IL-1 $\beta$ , exacerbating local inflammatory responses and contributing to tissue destruction and bone resorption. In contrast, M2 macrophages secrete anti-inflammatory factors, such as IL-1RA and IL-10, which mitigate inflammation and promote tissue repair. Studies have demonstrated that the M1/M2 macrophage ratio is typically elevated in periodontal tissues affected by periodontitis [6, 7], and reducing the M1/M2 ratio has been shown to alleviate the severity of the periodontitis [8]. Therefore, modulating macrophage polarization to decrease the proportion of M1 macrophages and enhance the function of M2 macrophages may represent an effective therapeutic strategy for treating periodontitis [9].

In recent years, mesenchymal stem cells (MSCs) have garnered significant attention for their potential in tissue repair and immunomodulation, making them widely applicable in the research and treatment of various autoimmune and inflammatory diseases [10–12]. MSCs can regulate macrophage polarization through mechanisms such as paracrine secretion of soluble factors, exosome release, metabolic reprogramming, and mitochondrial transfer, which inhibit the formation of M1 macrophages and promote M2 polarization, thereby alleviating local inflammatory responses and facilitating tissue repair [13, 14]. This immunomodulatory capability of MSCs offers new avenues for exploring their therapeutic applications in periodontitis.

Induced pluripotent stem cells (iPSCs) are a class of cells generated by reprogramming somatic cells (e.g., fibroblasts) into a pluripotent state [15]. iPSCs possess the ability to proliferate indefinitely in vitro and differentiate into nearly all cell types in the human body. Consequently, iPSCs hold immense potential in regenerative medicine, tissue engineering, and disease modeling. Moreover, as they are derived from somatic cells, their use circumvents the ethical concerns associated with embryonic tissues. iPSC-derived mesenchymal stem cells (iPSC-MSCs, abbreviated as iMSCs) are a subclass of MSCs generated through the directed differentiation of iPSCs. iMSCs inherit the multilineage differentiation potential and immunomodulatory capacity of traditional MSCs [16], while overcoming the limitations of source availability and quantity associated with traditional MSCs. As an emerging source of MSCs, iMSCs have gradually become a promising focus for research into autoimmune and inflammatory diseases [17]. Clinical trials have already reported the safety and efficacy of intravenous iPSC-MSC administration for steroid-resistant acute graft-versus-host disease [18], with two-year follow-up results further confirming the safety of iMSCs in therapeutic applications [19]. Additionally, iMSCs exhibit superior proliferative capacity compared to traditional MSCs [20, 21]. Unlike MSCs derived directly from bone marrow, adipose tissue, or other conventional sources, iMSCs provide a stable cell source that can be obtained through non-invasive methods, avoiding the traumatic procedures required for conventional MSC collection.

Furthermore, iMSCs are less influenced by donor age or health status. These advantages position iMSCs as a highly promising candidate for research into inflammatory diseases such as periodontitis and for applications in regenerative therapies.

Given the limited knowledge regarding the effects of iMSCs on macrophage polarization, this study investigated the regulatory role and underlying mechanisms of iMSCs in macrophage polarization within inflammatory environments. Furthermore, the therapeutic effects of iMSCs on ligature-induced periodontitis were explored. Our findings demonstrate that iMSCs inhibit M1 macrophage polarization through the NF- $\kappa$ B signaling pathway and mitigate alveolar bone loss in periodontitis.

## Methods

### Generation of MSCs from iPSCs (iMSCs)

The iPSCs employed in this study were previously reprogrammed and established from human peripheral blood mononuclear cells by our research group [22]. MSCs were derived from these iPSCs following a protocol described in a prior study [23], with minor modifications. Initially, iPSCs were seeded onto six-well plates pre-coated with Matrigel (Corning, USA) and cultured in PGM1 medium (Cellapy, China) until reaching approximately 80% confluency. Then, PGM1 medium was replaced with an MSCs induction medium, consisting of  $\alpha$ -MEM (Gibco, USA), 10% KnockOut™ Serum Replacement (Gibco, USA), 1% penicillin/streptomycin (EallBio, China), 1 mM sodium pyruvate (Gibco, USA), 50  $\mu$ M L-ascorbic acid (Sigma-Aldrich, USA), 2 mM L-glutamine (Gibco, USA), and 0.1 mM non-essential amino acids (Gibco, USA), with medium changes every two days over a 14-day period. Following this induction, cells were digested with 0.25% trypsin (EallBio, China) and then seeded onto 10 cm culture dishes coated with 0.1% gelatin, denoted as passage 1 (P1) iMSCs, where the gelatin coating was applied only for the first two passages. From P1 onwards, cells were cultured and expanded in MSCs maintenance medium A, which contained high-glucose DMEM (EallBio, China), 10% fetal bovine serum (FBS; EallBio, China), 5 ng/mL basic fibroblast growth factor (PeproTech, USA), and 10 ng/mL epidermal growth factor (PeproTech, USA), with continued passaging. Passaging ceased at P3, with medium replacement every three days. After 3–5 weeks, large clusters of cells with the characteristic MSCs morphology appeared. Cells from P4 onward were considered successfully differentiated MSCs, maintained in MSCs maintenance medium B containing high-glucose DMEM with 10% FBS for subsequent expansion

and passaging. For functional experiments, iPSC-MSCs at passages 5–10 were employed.

### Trilineage differentiation of iMSCs

For osteogenic induction differentiation, cells were cultured for 21 days in osteogenic induction medium comprising  $\alpha$ -MEM, 10% FBS, 50  $\mu$ M L-Ascorbic acid (Sigma-Aldrich, USA), 0.1  $\mu$ M dexamethasone (Solarbio, China), 10 mM  $\beta$ -glycerophosphate (Sigma-Aldrich, USA), and 1% penicillin–streptomycin. Cells were stained with 1% Alizarin Red S solution (Solarbio, China) to confirm mineral deposition. For adipogenic differentiation, high-glucose DMEM containing 10% FBS, 0.5  $\mu$ M 3-isobutyl-1-methylxanthine (Sigma-Aldrich, USA), 0.5  $\mu$ M dexamethasone, 10  $\mu$ g/mL insulin (Sigma-Aldrich, USA), 50  $\mu$ M indomethacin (Sigma-Aldrich, USA), and 1% penicillin–streptomycin was used as the adipogenic induction medium. Cells were cultured in this medium for 21 days, stained with Oil Red O staining (Solarbio, China) to detect lipid droplet formation. For chondrogenic differentiation, cells were cultured for 21 days in chondrogenic induction medium containing DMEM, 10% FBS, 0.1  $\mu$ M dexamethasone, 1 mM sodium pyruvate (Sigma-Aldrich, USA), 40  $\mu$ g/mL proline (Sigma-Aldrich, USA), 10 ng/mL TGF- $\beta$ 1 (PeproTech, USA), and 50  $\mu$ g/mL L-Ascorbic acid. Following this period, Alcian Blue staining (Solarbio, China) was performed to visualize chondrogenic differentiation. Conventionally cultured iMSCs were used as controls and subjected to the corresponding staining procedures.

### Polarization of macrophages and co-cultures with iMSCs

Human monocytic THP-1 cells, purchased from EallBio (Beijing, China), was maintained in RPMI 1640 medium (Gibco, USA) supplemented with 10% fetal bovine serum (FBS), 1% penicillin/streptomycin, and 0.05 nM 2-mercaptoethanol (Gibco, USA) at 37 °C in a 5% CO<sub>2</sub> incubator. The medium was replaced every other day, and the cells were passaged every four days. To induce differentiation into M0 macrophages, THP-1 cells were exposed to 100 ng/mL Phorbol 12-Myristate 13-Acetate (PMA, Sigma-Aldrich, USA) for 48 h. Subsequently, PMA was removed by medium exchange, and M0 macrophages were polarized into the M1 phenotype by incubation with 20 ng/mL IFN- $\gamma$  (MCE, USA) and 100 ng/mL LPS from *P. gingivalis* (InvivoGen, France) for an additional 48 h (M0 + LPS + IFN- $\gamma$  group).

For the co-culture of macrophages with iMSCs, THP-1 cells were seeded at a density of  $1 \times 10^6$  cells per well in six-well plates and differentiated into M0 macrophages using PMA. iMSCs ( $2.5 \times 10^5$ ) were then plated in the upper chamber of Transwell inserts (0.4  $\mu$ m pore size, NEST, China) to establish a co-culture

system. LPS and IFN- $\gamma$  were added to the system to sustain the macrophage activation process for 48 h (M0+LPS+IFN- $\gamma$ +iMSCs group). Conditioned medium (CM), RNA, and protein from macrophages under various conditions were collected for subsequent analyses.

#### **The osteogenic differentiation of periodontal ligament stem cells (PDLSCs)**

Human PDLSCs were purchased from EallBio (Beijing, China) and cultured in  $\alpha$ -MEM medium (Gibco, USA) supplemented with 10% fetal bovine serum (FBS) and 1% penicillin/streptomycin. PDLSCs at a density of  $1 \times 10^5$  cells per well were seeded into 12-well plates, and osteogenic differentiation was induced using a 3:1 mixture of osteogenic induction medium and macrophage-conditioned medium (CM), with medium changes performed every three days. After seven days of differentiation, the cells were fixed in 4% paraformaldehyde (EallBio, China) for 30 min and stained using the BCIP/NBT ALP color development kit (Beyotime, China). Alkaline phosphatase (ALP) activity was measured using the Alkaline Phosphatase Assay Kit (Beyotime, China). After 21 days of induction, the cells were fixed and stained with 1% Alizarin Red S solution (Solarbio, China) to identify mineralized nodules. The stained nodules were subsequently dissolved in 10% cetylpyridinium chloride solution (Aladdin, China), and the absorbance was measured at 562 nm using a microplate reader (Molecular Devices, USA). RNA samples were collected on days 7 and 21 for real-time quantitative polymerase chain reaction (RT-qPCR) analysis.

#### **Cytokine analysis**

In addition to the aforementioned co-culture system, an iMSCs+LPS+IFN- $\gamma$  group was established to determine cytokine levels secreted by iMSCs under inflammatory conditions. Specifically, iMSCs ( $2.5 \times 10^5$ ) were seeded into the upper chamber of Transwell inserts, and LPS and IFN- $\gamma$  were added for further 48-h culture (iMSCs+LPS+IFN- $\gamma$  group). The quantification of cytokines was performed using a 27-plex magnetic bead-based immunoassay kit (Bio-Rad, M500KCAF0Y, USA) in accordance with the manufacturer's instructions. The concentrations of 27 cytokines in the supernatants of macrophages from the M0 group, M0+LPS+IFN- $\gamma$  group, M0+LPS+IFN- $\gamma$ +iMSCs group, and iMSCs+LPS+IFN- $\gamma$  group were analyzed. The detection was conducted using the Luminex X-200 system (Luminex Corporation, USA), and data analysis was performed with Milliplex Analyst software (Version

5.1, Merck Millipore, USA). The intra-assay and inter-assay coefficients of variation (CV) were confirmed to be below 15%, ensuring the reproducibility of the measurements. Cytokine concentrations were expressed in picograms per milliliter (pg/mL).

#### **Detection of intracellular reactive oxygen species (ROS)**

The levels of ROS in macrophages were measured using a ROS detection kit (Beyotime, China). Following a 12-h stimulation with LPS and IFN- $\gamma$  or co-culture with iMSCs, cells were incubated with 2 mL of 0.1% dichlorofluorescein diacetate (DCFH-DA) at 37 °C for 30 min. Rosup (50  $\mu$ g/mL) was used as a positive control for ROS induction. The cells were then washed with serum-free RPMI 1640 medium to remove excess DCFH-DA. Subsequently, the cells were observed and imaged under a fluorescence microscope. Following fluorescence imaging, the cells were detached using Accutase (Sigma-Aldrich, USA) and subjected to flow cytometry to quantify ROS levels. The mean fluorescence intensity (MFI) in the FITC channel was used as a quantitative indicator of ROS production.

#### **Flow cytometry analysis**

The immunophenotypic characterization of iMSCs was performed following the ISCT standards [24]. iMSCs were digested using trypsin and stained with the following antibodies at 4 °C for 30 min: CD73-APC (BioLegend, USA), CD90-FITC (BioLegend, USA), CD146-PE (BioLegend, USA), CD105-PE (BioLegend, USA), CD34-PE (BD Biosciences, USA), CD45-PE (BioLegend, USA), and HLA-DR-APC (BioLegend, USA).

For the detection of M1 macrophages marker CD86 and M2 macrophages marker CD206, cells were incubated with CD11b-FITC (BioLegend, USA) and CD86-PE antibodies (BioLegend, USA) in the dark for 30 min. After centrifugation, cells were fixed and permeabilized using BD Cytfix/Cytoperm (BD Biosciences, USA) according to the manufacturer's protocol, followed by incubation with CD206-APC antibody (BioLegend, USA) at 4 °C for 30 min.

For ROS detection by flow cytometry, macrophages were harvested by digestion with Accutase for 15 min and washed twice with PBS. ROS levels were quantified using the FITC channel, with the mean fluorescence intensity of FITC serving as the indicator.

Flow cytometry was performed using a CytoFLEX S flow cytometer (Beckman Coulter, USA), and data were analyzed with CytExpert software (version 2.6, Beckman Coulter, USA).



**Reverse transcription-quantitative polymerase chain reaction (RT-qPCR) analysis**

Total RNA was extracted from cells using TRIzol reagent (Invitrogen, USA), and cDNA was synthesized through reverse transcription using the TaKaRa PrimeScript RT Reagent Kit (Takara Biomedical Technology, Japan). RT-qPCR was performed with the SYBR Green Pro Taq HS qPCR Kit (AG, China) on the AriaMx Real-Time PCR System (Agilent, USA). Data were analyzed using the comparative  $\Delta\Delta C_t$  method, with GAPDH serving as the internal control. The primer sequences for the target genes are listed in Table 1.

**Western blot analysis**

Total protein was extracted using a Protease Inhibitor Cocktail (TargetMol, USA), Phosphatase Inhibitor Cocktail III (TargetMol, USA), and RIPA Lysis Buffer (Applygen, China). Protein samples were loaded and separated by electrophoresis on a 10% SDS-PAGE gel (EPIZYME, China). The separated proteins were transferred onto a PVDF membrane (Merck Millipore, USA). The membrane was blocked for 30 min with a Rapid Blocking Buffer (EPIZYME, P2108P) and incubated overnight at 4 °C with primary antibodies. After three washes with TBST, the membrane was incubated with the secondary antibody for 1 h. Immunoreactive bands were visualized using the Immobilon ECL Ultra Western HRP substrate (Merck Millipore, USA). The primary antibodies used were as follows: Nrf2 (1:1000, Abmart, China),

HO-1 (1:1000, Abmart, China), NQO1 (1:1000, Abmart, China), AKT (1:1000, Abmart, China), P-AKT (1:1000, Abmart, China), NF- $\kappa$ B p65 (1:1000, Abmart, China), P-NF- $\kappa$ B p65 (1:1000, Abmart, China), GAPDH (1:3000, Abclonal, China), and  $\beta$ -tubulin (1:2000, Abmart, China).

**Transcriptomic analysis**

RNA sequencing and bioinformatics analysis were conducted with the assistance of NovelBio BioPharm Technology Co., Ltd (Shanghai, China). Total RNA was extracted from macrophages under four conditions: M0, M0 co-cultured with iMSCs in a Transwell system (M0+iMSCs), M0 stimulated with LPS and IFN- $\gamma$  (M0+LPS+IFN- $\gamma$ ), and M0 stimulated with LPS and IFN- $\gamma$  in the presence of iMSCs (M0+LPS+IFN- $\gamma$ +iMSCs). The cDNA libraries for each RNA sample were prepared using the VAHTS Universal V6 RNA-seq Library Prep Kit for Illumina (Vazyme, China) following the manufacturer's instructions. The libraries underwent quality control using the Agilent 2200 system and were sequenced on the DNBSEQ-T7 platform with 150 bp paired-end reads. Clean reads were obtained by removing adapter sequences and low-quality reads from the raw data. Differentially expressed genes (DEGs) were identified using the DESeq2 algorithm [25] based on the following criteria: (i) Fold Change > 2 or < 0.5, (ii) *P*-value < 0.05, and (iii) FDR < 0.05 [26]. Gene Ontology (GO) analysis and Pathway Analysis were performed using the CytoNavigator™ RNA-Seq Analysis Platform. GO annotations data were sourced from NCBI (<http://www.ncbi.nlm.nih.gov/>), UniProt (<http://www.uniprot.org/>), and Gene Ontology (<http://www.geneontology.org/>), and significant GO categories were identified using Fisher's exact test (*P*-value < 0.05). Pathway analysis was conducted based on the KEGG database to identify significant pathways associated with the DEGs, with Fisher's exact test applied to determine statistical significance (*P*-value < 0.05).

**Ligature-induced periodontitis mouse model**

The work has been reported in line with the ARRIVE guidelines 2.0. Male C57BL/6 mice aged 4–6 weeks were purchased from the Experimental Animal Center of Peking University Health Science Center. All mice were housed in the same facility under specific pathogen-free conditions, maintained on a 12-h light/dark cycle. The experimental protocol was approved by the Biomedical Ethics Committee of Peking University (Approval No.: PUIRB-LA2023075). The mice were randomly assigned to three groups: healthy control group (*n*=5), untreated periodontitis group (*n*=5), and periodontitis group treated with iMSCs (*n*=5). Mice in the healthy control group received no treatment. In the untreated

**Table 1** Primer sequences used for qRT-PCR

Gene	Forward primer	Reverse primer
GAPDH	ATCAAGAAGGTGGTGAAGCAGG	GTCATACCAGGAAATGAGC
IL-1 $\beta$	ACGATGCACCTGTACGATCA	TCTTTCAACACGCAGGACAG
TNF- $\alpha$	CCCAGGGACCTCTCTCTAATCA	GCTTGAGGGTTTGCTACAACATG
iNOS	CGCATGACCTTGGTGTGTTGG	CATAGACCTTGGGCTTGCCA
IL-10	GTGATGCCCAAGCTGAGA	CACGGCCTTGCTCTTGTTTT
Arg-1	CTTGGCAAAAGACTTATCTTAG	ATGACATGGACACATAGTACCTTTC
CAT	GTGCGGAGATTCAACACTGCCA	CGGCAATGTTCTCACACAGACG
HO-1	CCAGGCAGAGAATGCTGAGTTC	AAGACTGGGCTCTCCTTGTTGC
NQO1	CCTGCCATTCTGAAAGGCTGGT	GTGGTGATGGAAAGCACTGCCT
ALP	CTTGACCTCTCGGAAGACAC	CAGACCAAAGATAGAGTTGCCAC
OCN	CTCACACTCTCGCCCTATTG	GGTCTCTTCACTACCTCGTGCG
RUNX2	CCATAACCGTCTTCACAAATCC	GTTCCCGAGGTCCACTACTG
COL-1	AGAACAGCGTGGCCT	TCCGGTGACTCGT

periodontitis group, experimental periodontitis was induced under sodium pentobarbital anesthesia by placing a 5–0 silk ligature around the cervical region of the second maxillary molars bilaterally. In the iMSC-treated periodontitis group, ligatures were placed as described above, and mice received local periodontal injections of iMSCs ( $5 \times 10^5$  cells suspended in 10  $\mu$ L PBS) on days 3, 5, 7, and 10. After two weeks, the mice were euthanized by cervical dislocation, and the maxillae were harvested and fixed in 4% paraformaldehyde for 24 h for subsequent analyses. The personnel conducting the experiments were not involved in the result analysis, and two independent researchers cross-verified the analysis outcomes.

#### Micro-CT analysis

Micro-CT (Siemens Medical Solutions USA, Inc., Hoffman Estates, IL, USA) was used to assess alveolar bone loss. Scanning was performed with a resolution of 10  $\mu$ m. Upon completion of the scan, image data were exported, and quantitative analysis was conducted on parameters such as bone mineral density (BMD) and bone volume/total volume ratio (BV/TV) to evaluate changes in the alveolar bone. Bone morphological changes in the alveolar bone were further validated using Mimics software (Materialise, Belgium), and the distance between the cemento-enamel junction (CEJ) and alveolar bone crest (AB) of the maxillary second molar was measured and presented.

#### Histological analysis

The maxillae of mice were decalcified in 10% EDTA solution for two weeks, followed by the preparation of 4- $\mu$ m-thick paraffin sections for HE staining. TRAP staining: After deparaffinization, sections were stained using a TRAP staining kit (Servicebio, GB1050, China), dehydrated, and mounted. Immunofluorescence staining: Sections were deparaffinized, hydrated, subjected to antigen retrieval, and blocked for endogenous peroxidase activity. The sections were then blocked with bovine serum albumin and incubated overnight at 4 °C with primary antibodies against CD68 (Servicebio, GB113109, 1:100), iNOS (Servicebio, GB11119, 1:100), CD206 (Servicebio, GB113497, 1:100), and p65 (Bioss, BS-0465R, 1:100). For secondary antibody staining,

sections labeled with CD68, iNOS, and CD206 were incubated with a green fluorescent secondary antibody (Servicebio, GB22303, 1:100), while sections labeled with p65 were incubated with a red fluorescent secondary antibody. Nuclei were counterstained with DAPI, and slides were mounted using an anti-fade mounting medium. Immunohistochemical (IHC) staining: Sections were deparaffinized and hydrated, followed by antigen retrieval. After blocking with bovine serum albumin (BSA), tissue sections were incubated overnight at 4 °C with the primary antibody against IL-17A (Proteintech, 1:100). After washing, sections were treated with a secondary antibody (Servicebio, GB23303, 1:100), developed with DAB chromogen, counterstained with hematoxylin for 1 min to label nuclei, and finally dehydrated and mounted. IHC, HE and TRAP-stained sections were scanned using a WISLEAP WS-10 pathological slide scanner (WISLEAP, China). Immunofluorescence images were captured using a confocal fluorescence microscope, and both TRAP-stained and immunofluorescence images were analyzed using ImageJ software.

#### Statistical analysis

All data are presented as the mean  $\pm$  standard deviation. Western blot bands, TRAP staining, immunohistochemistry, and immunofluorescence images were analyzed using ImageJ (version 1.53e, National Institutes of Health, USA). Graphs and statistical analyses were performed using GraphPad Prism (version 8.0.2, GraphPad Software Inc., USA). One-way analysis of variance (ANOVA) was used for multiple group comparisons. A *P*-value of  $<0.05$  was considered statistically significant.

## Results

#### Characterization of iMSCs

After 14 days of induced differentiation, iPSCs with typical colony morphology transformed into numerous spindle-shaped cells, and fully differentiated iMSCs exhibited the characteristic fibroblast-like spindle morphology (Fig. 1A). Alizarin Red S staining for calcium deposition, Oil Red O staining for lipid droplets, and Alcian Blue staining for cartilage matrix were performed to assess osteogenic, adipogenic, and chondrogenic differentiation,

(See figure on next page.)

**Fig. 1** Characterization of iMSCs Morphology, Differentiation Potential, and Cell Surface Markers. **A** The left panel shows the typical colony morphology of iPSCs, the middle panel illustrates the morphological changes of iPSCs after 14 days of induced differentiation, and the right panel depicts the characteristic morphology of mesenchymal stem cells in P5 generation iMSCs. **B** Results of Alizarin Red S staining for calcium deposition, Oil Red O staining for lipid droplets, and Alcian Blue staining for cartilage matrix. **C** Flow cytometry analysis showing the expression of cell surface markers on iMSCs

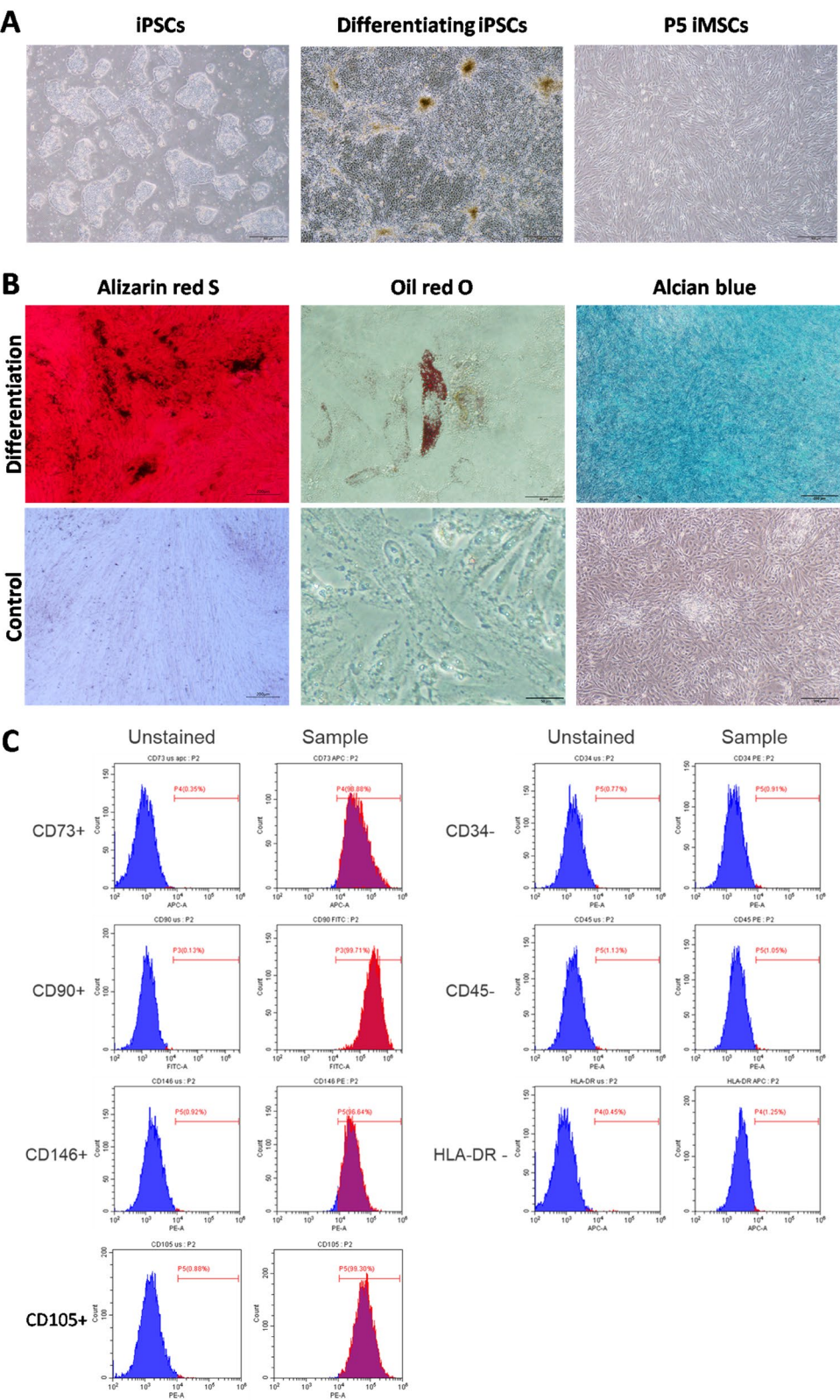


**Fig. 1** (See legend on previous page.)



respectively. Positive staining results confirmed the tri-lineage differentiation potential of iMSCs (Fig. 1B). Flow cytometry analysis revealed that iMSCs expressed typical MSC surface markers, including CD73, CD90, CD105, and CD146, while showing negative expression for CD34 and CD45 (Fig. 1C). These results demonstrate that iMSCs meet the identification criteria for mesenchymal stem cells as defined by the International Society for Cellular Therapy [24].

### iMSCs inhibit M1 polarization of macrophages

THP-1 cells were stimulated with PMA to differentiate from a suspension state into adherent M0 macrophages with a rounded morphology. After removing PMA for 48 h, M0 macrophages exhibited a spindle-shaped or oval morphology (Fig. 2A). Following stimulation with LPS and IFN- $\gamma$  for 48 h, the M0 macrophages were further polarized into M1 macrophages under PMA-free conditions, displaying a more irregular morphology with extended short pseudopodia (Fig. 2A). To investigate the regulatory effects of iMSCs on macrophages in vitro, iMSCs were indirectly co-cultured with macrophages in a Transwell system for 48 h. In the presence of iMSCs, the macrophages exhibited intermediate characteristics. While some cells retained the activated morphology observed in the LPS+IFN- $\gamma$  group, many cells appeared to revert to a more elongated morphology resembling that of the M0 group (Fig. 2A). CD11b was used as a general macrophage surface marker, CD86 as an M1 macrophage marker, and CD206 as an M2 macrophage marker. Flow cytometry analysis revealed that in the presence of LPS and IFN- $\gamma$ , iMSCs significantly reduced the proportion of CD86+/CD11b+ M1 macrophages from 41.61 to 16.85% (Fig. 2B), a difference that was statistically significant (Fig. 2D), indicating that co-culture with iMSCs effectively inhibited the polarization of M0 macrophages into the M1 phenotype under inflammatory conditions. In contrast, the proportion of CD206+/CD11b+ M2 macrophages showed no significant difference among the groups (Fig. 2C, E), suggesting that iMSCs had a limited effect on M2 polarization under LPS+IFN- $\gamma$  stimulation conditions. At the mRNA

level, co-culture with iMSCs significantly downregulated the expression of pro-inflammatory cytokines interleukin-1 beta (IL-1 $\beta$ ) and tumor necrosis factor-alpha (TNF- $\alpha$ ), while markedly upregulating the expression of anti-inflammatory factors interleukin-10 (IL-10) and arginase-1 (Arg-1), compared to the M0+LPS+IFN- $\gamma$  group (Fig. 2F).

### iMSCs alleviate oxidative stress in macrophages under inflammatory conditions

Previous studies have suggested that iMSCs possess the potential to mitigate oxidative stress [27], but the underlying mechanisms remain unclear. Given the close association between macrophage inflammatory responses and oxidative stress, we investigated the effects of iMSCs on macrophage oxidative stress. The effect of iMSCs on ROS release levels in macrophages was assessed under LPS and IFN- $\gamma$  stimulation. Using M0+Rosup as the positive control group, LPS and IFN- $\gamma$  treatment significantly increased ROS release in macrophages compared to the M0 group, whereas co-culture with iMSCs markedly reduced ROS levels in macrophages (Fig. 3A). Quantification of ROS fluorescence intensity via flow cytometry revealed that the M0+LPS+IFN- $\gamma$  group exhibited the strongest fluorescence signals, while the co-culture group displayed a reduction in fluorescence intensity, nearing the levels observed in the M0 group (Figs. 3B, C).

Next, we assessed the relative expression of antioxidant genes (CAT, HO-1, and NQO1) in macrophages. At 24 h, LPS+IFN- $\gamma$  treatment suppressed the expression of CAT and NQO1 as expected, whereas co-culture with iMSCs significantly upregulated NQO1 expression, despite further suppressing CAT and HO-1 expression (Fig. 3D). At 48 h, HO-1 expression was markedly increased in the M0+LPS+IFN- $\gamma$  group and reduced upon co-culture with iMSCs; CAT expression was significantly higher in the M0+LPS+IFN- $\gamma$ +iMSCs group compared to other groups, while NQO1 expression showed no significant differences among the three groups (Fig. 3D). The differential expression of these antioxidant genes at 24 and 48 h indicates a temporal pattern of antioxidant gene regulation. Catalase (CAT), encoded by the CAT gene,

(See figure on next page.)

**Fig. 2** The inhibitory effects of iMSCs on M1 macrophage polarization (induced by LPS and IFN- $\gamma$ ) analyzed through morphological, flow cytometric, and gene expression assessments. **A** Representative images of THP-1 cells and macrophages under different conditions. From left to right: THP-1 cells stimulated with PMA for 48 h, M0 macrophages cultured in PMA-free medium for 48 h, M1 macrophages induced with LPS and IFN- $\gamma$ , and M1 macrophages co-cultured with iMSCs. Scale bar: 100  $\mu$ m. **B** Flow cytometry of M1 macrophage polarization. The upper-right quadrant indicates the proportion of CD11b+/CD86+ M1 macrophages. **C** Flow cytometry of M2 macrophage polarization. The upper-right quadrant shows the proportion of CD11b+/CD206+ M2 macrophages. **D** Quantitative flow cytometry analysis illustrating significant differences in the proportion of CD86+/CD11b+ cells between treatment groups. **E** Quantitative flow cytometry analysis indicating no significant differences in the proportion of CD206+/CD11b+ cells among the groups. **F** Expression of macrophage inflammatory and anti-inflammatory marker genes, including IL-1 $\beta$ , TNF- $\alpha$ , iNOS, IL-10, and Arg-1. \* $P$  < 0.05, \*\* $P$  < 0.01, \*\*\* $P$  < 0.001; ns, not significant ( $P$  > 0.05)



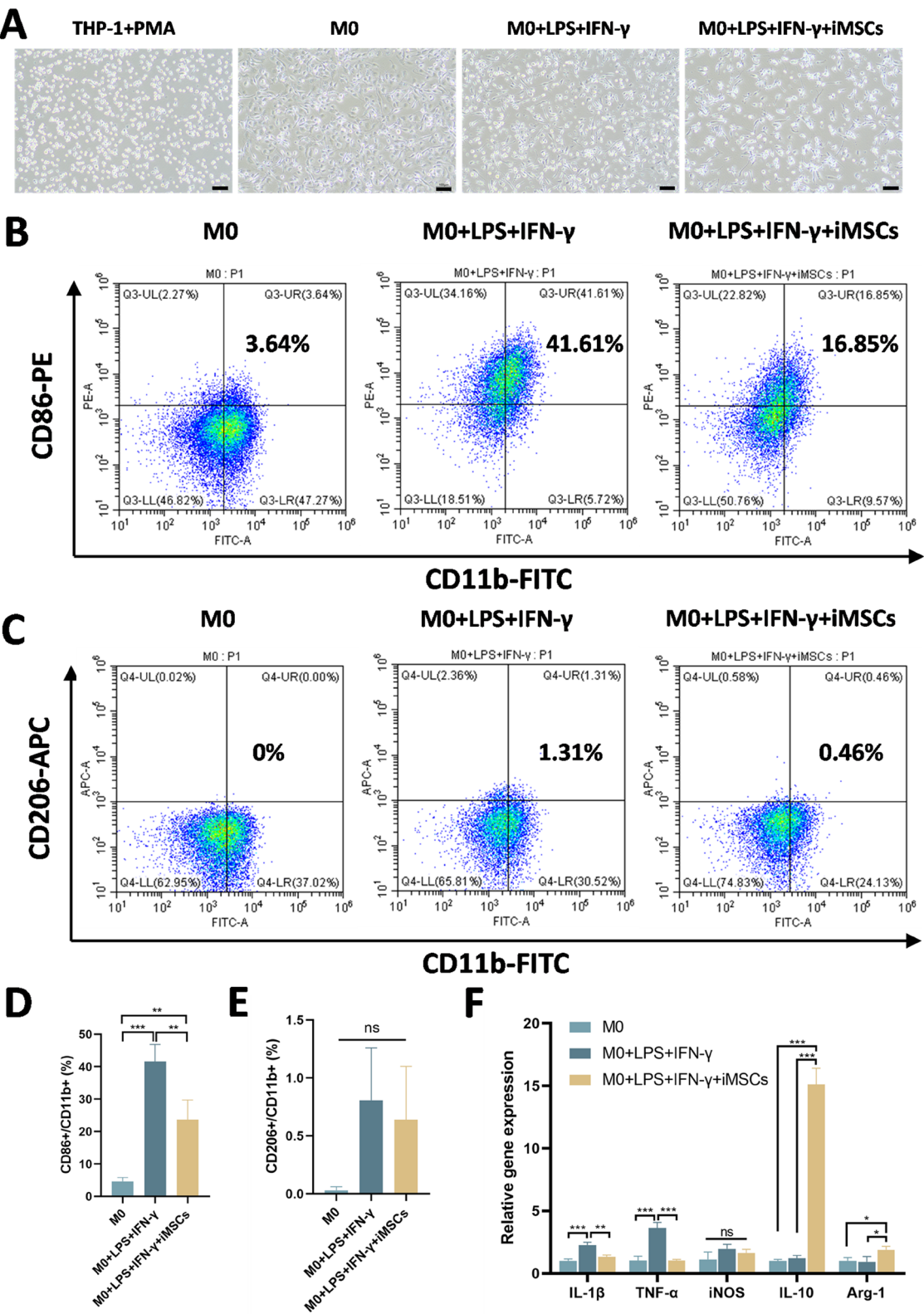


**Fig. 2** (See legend on previous page.)

protects cells from oxidative damage by decomposing hydrogen peroxide. NAD(P)H Quinone Dehydrogenase 1 (NQO1), an antioxidant enzyme, maintains redox homeostasis and reduces free radical and ROS generation [28]. In the M0+LPS+IFN- $\gamma$ +iMSCs group, CAT expression initially decreased at 24 h but subsequently increased at 48 h, while NQO1 expression was upregulated only at 24 h, indicating distinct temporal patterns in their antioxidative responses. Interestingly, the expression of haem oxygenase-1 (HO-1) in the M0+LPS+IFN- $\gamma$  group, as anticipated, decreased at 24 h but exhibited a significant upregulation at 48 h. HO-1 is a stress-inducible enzyme [29], and this marked upregulation at 48 h might be attributed to pronounced oxidative stress induced in macrophages by LPS and IFN- $\gamma$  stimulation. Moreover, it has been reported that HO-1 does not always exert antioxidative effects; in certain circumstances, overexpression of HO-1 has been shown to exhibit pro-oxidative properties [29–32], which could also explain the observed upregulation at 48 h. Similarly, co-culture with iMSCs enhanced the protein levels of NQO1 while reducing HO-1 protein levels compared to the M0+LPS+IFN- $\gamma$  group (Fig. 3E, F), a trend consistent with the gene expression patterns of HO-1 and NQO1 observed at 24 h. No significant differences were found in Nrf2 protein levels among the three groups, suggesting that the time point chosen for analysis might not coincide with the regulatory effects of Nrf2 on oxidative stress.

Overall, iMSCs effectively attenuated ROS release in macrophages under inflammatory conditions by upregulating the transcription of antioxidant genes, such as NQO1 and CAT, and increasing NQO1 protein expression, thereby significantly mitigating oxidative stress induced by LPS and IFN- $\gamma$ .

### The effects of iMSCs on cytokine secretion by macrophages under inflammatory conditions

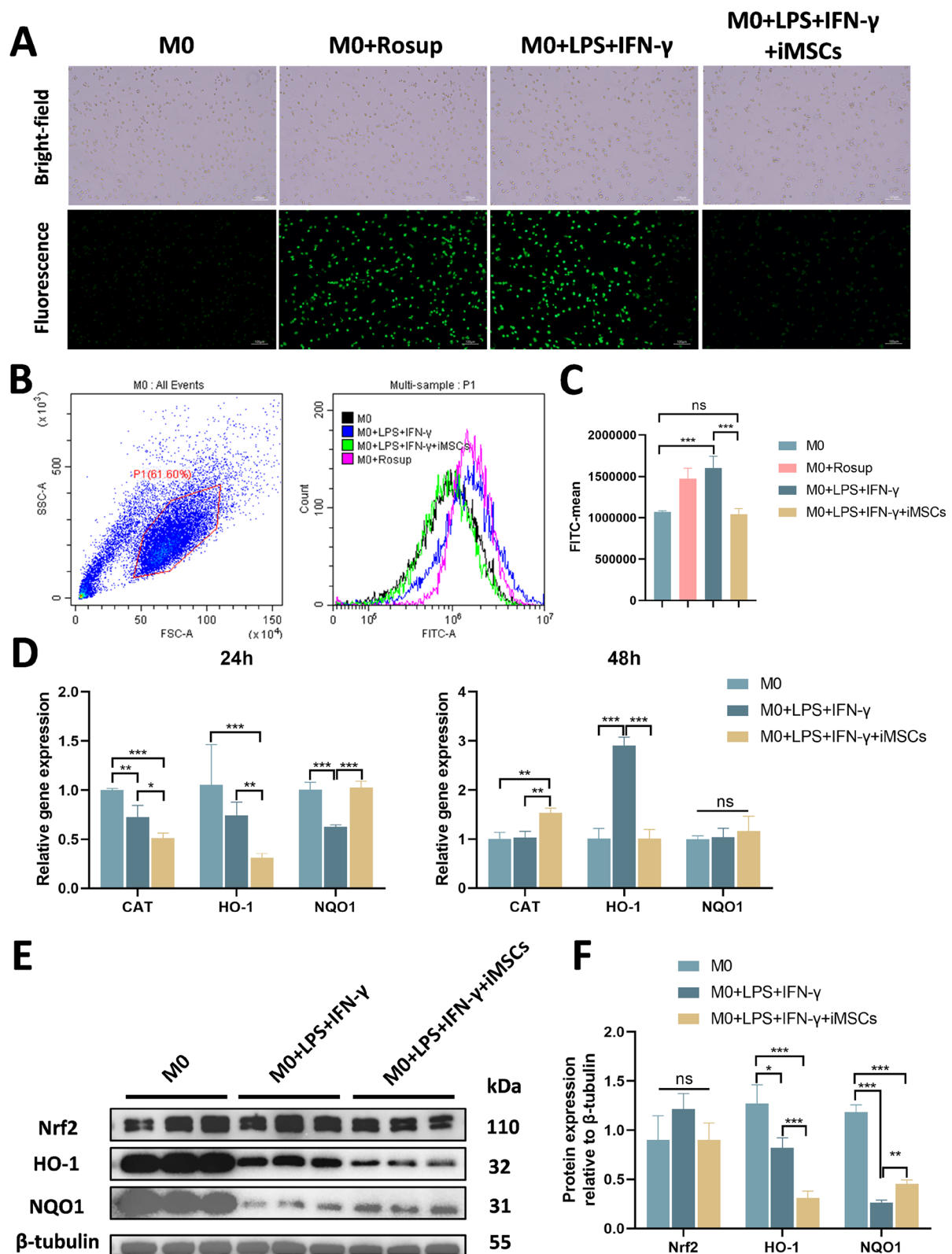
Considering the critical role of cytokines in macrophage polarization. Multiplex Bead-Based Immunoassay was employed to analyze the impact of iMSCs co-culture on the secretion of 27 soluble cytokines by macrophages stimulated with LPS+IFN- $\gamma$  (Fig. 4). Due to exceeding

the detection limit, IL-6, MIP-1 $\beta$ , and IP-10 were excluded from the results. The remaining 24 cytokines were categorized into pro-inflammatory cytokines (IFN- $\gamma$ , IL-12p70, TNF- $\alpha$ , IL-1 $\beta$ , IL-17), anti-inflammatory cytokines (IL-1ra, IL-4, IL-10, IL-13), growth factors (bFGF, PDGF-BB, VEGF), colony-stimulating factors (G-CSF, GM-CSF), chemokines (RANTES, Eotaxin, MCP-1, MIP-1 $\alpha$ , IL-8), and immune-related cytokines (IL-2, IL-5, IL-7, IL-9, IL-15), which collectively regulate inflammatory responses, immune cell activation, chemotaxis, and tissue repair. The cytokines secreted by the M0+LPS+IFN- $\gamma$ +iMSCs group originate from both macrophages and iMSCs. To quantitatively assess macrophage-derived cytokines in the co-culture system, we measured cytokines released by LPS+IFN- $\gamma$ -stimulated iMSCs (LPS+IFN- $\gamma$ +iMSCs group). The macrophage-specific cytokine contribution in the co-culture group was calculated by subtracting the cytokine levels of the LPS+IFN- $\gamma$ +iMSCs group from those of the M0+LPS+IFN- $\gamma$ +iMSCs group. Notably, with the exception of MCP-1, cytokine levels produced by LPS+IFN- $\gamma$ -stimulated iMSCs (LPS+IFN- $\gamma$ +iMSCs group) were dramatically lower (by orders of magnitude) compared to both the M0+LPS+IFN- $\gamma$  group and the M0+LPS+IFN- $\gamma$ +iMSCs group. Consequently, it is reasonable to approximate that the cytokine profile of the M0+LPS+IFN- $\gamma$ +iMSCs group predominantly reflects macrophage-derived cytokines in the co-culture system.

Under LPS+IFN- $\gamma$  treatment, iMSCs co-culture modulated cytokine secretion by macrophages (Fig. 4), while results demonstrating no effect of iMSCs on cytokine secretion are provided in the supplementary file (Suppl. Figure 3). LPS+IFN- $\gamma$  stimulation significantly enhanced the secretion of pro-inflammatory cytokines by macrophages (Fig. 4A, Suppl. Figure 3A), while iMSCs co-culture significantly reduced the levels of IL-1 $\beta$  and IL-17 (Fig. 4A). Interestingly, anti-inflammatory cytokines such as IL-1ra, IL-4, IL-10, and IL-13 were also notably increased under LPS+IFN- $\gamma$  stimulation (Fig. 4B, Suppl. Figure 3B). Co-culture with iMSCs further elevated IL-10 levels while reducing IL-4 levels (Fig. 4B). IL-10 is a key cytokine in suppressing inflammation and regulating immune responses, widely regarded as a core

(See figure on next page.)

**Fig. 3** The regulatory effects of iMSCs on oxidative stress levels and the expression of antioxidant genes and proteins in macrophages stimulated with LPS+IFN- $\gamma$ . **A** ROS levels in macrophages were visualized using dichlorofluorescein diacetate staining, with bright-field and fluorescence microscopy imaging. **B** Flow cytometry analysis of fluorescence intensity in the FITC channel was performed to assess ROS levels across different treatment groups, with the left panel showing gating strategy and the right panel displaying fluorescence intensity distributions for each group. **C** Quantification of ROS levels was assessed by measuring the mean fluorescence intensity (FITC-mean) using flow cytometry. **D** The relative expression levels of antioxidant genes (CAT, HO-1, NQO1) in macrophages were determined by RT-qPCR at 24 and 48 h. **E** Protein expression levels of Nrf2, HO-1, and NQO1 were analyzed via Western blot (Full-length blots are presented in Supplementary Fig. 2A–D). **F** Quantitative analysis of Nrf2, HO-1, and NQO1 protein levels was conducted relative to  $\beta$ -tubulin expression. \* $P$ <0.05, \*\* $P$ <0.01, \*\*\* $P$ <0.001; ns, not significant ( $P$ >0.05)



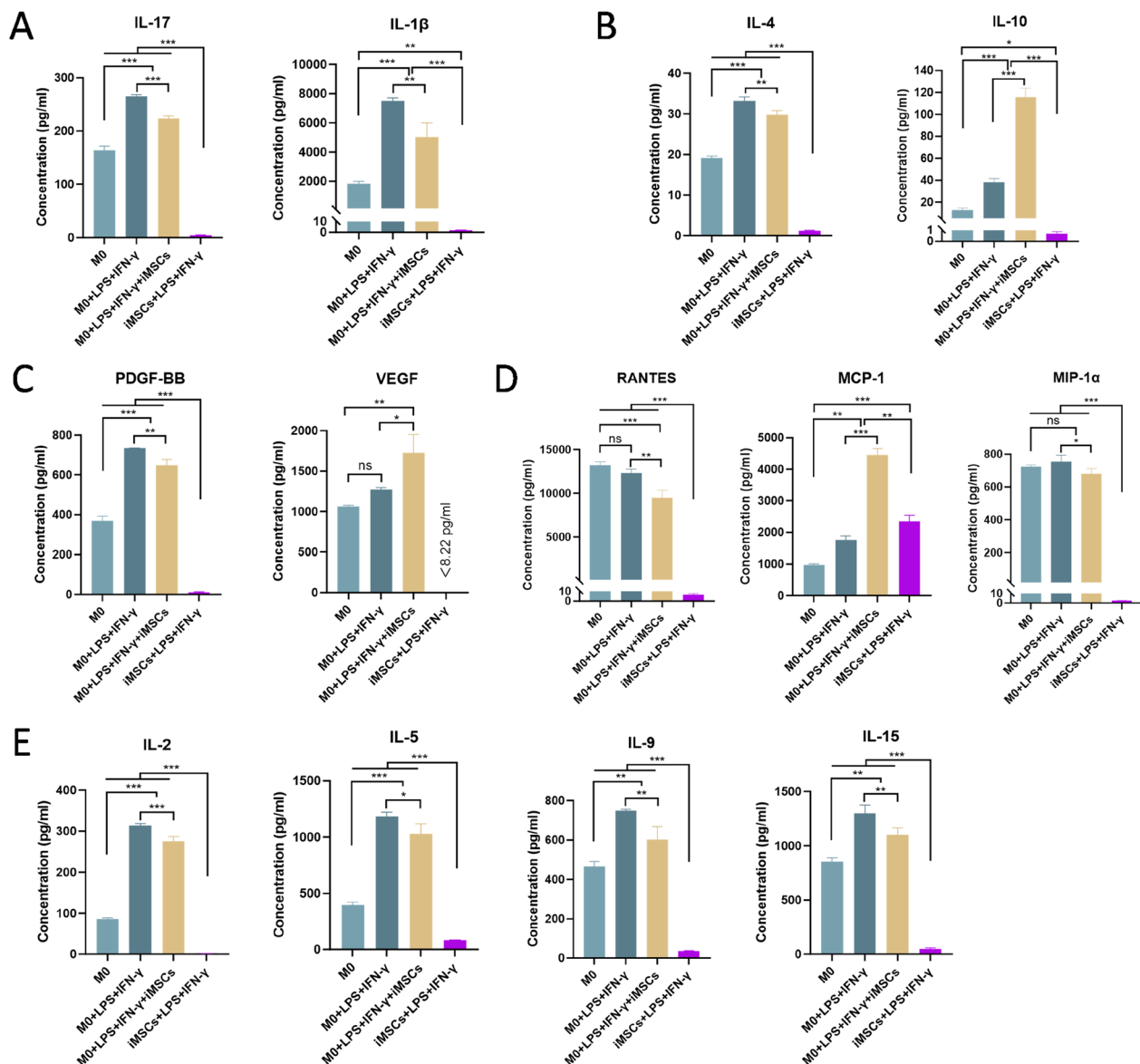


**Fig. 4** The concentration changes of cytokines secreted by macrophages under different treatment conditions (M0, M0+LPS+IFN- $\gamma$ , M0+LPS+IFN- $\gamma$ +iMSCs, and iMSCs+LPS+IFN- $\gamma$ ). **A** Pro-inflammatory cytokines (IL-1 $\beta$ , IL-17). **B** Anti-inflammatory cytokines (IL-4, IL-10). **C** Growth factors (PDGF-BB, VEGF). **D** Chemokines (RANTES, MCP-1, MIP-1 $\alpha$ ). **E** Immune-related cytokines (IL-2, IL-5, IL-9, IL-15). Each bar chart represents the concentration of an individual cytokine (pg/ml). \* $P < 0.05$ , \*\* $P < 0.01$ , \*\*\* $P < 0.001$ ; ns, not significant ( $P > 0.05$ )

factor in anti-inflammatory mechanisms [33]. Despite the downregulation of IL-4, iMSCs may predominantly exert their anti-inflammatory effects predominantly through the upregulation of the core anti-inflammatory cytokine IL-10.

Growth factors are involved in tissue repair and regeneration. Basic FGF and PDGF-BB were significantly elevated in both the M0+LPS+IFN- $\gamma$  group and the M0+LPS+IFN- $\gamma$ +iMSCs group (Fig. 4C, Suppl. Figure 3C), whereas VEGF showed a significant increase

only in the LPS+IFN- $\gamma$ +iMSCs group (Fig. 4C). It indicates that iMSCs co-culture significantly enhances VEGF secretion by macrophages under LPS+IFN- $\gamma$  stimulation. For colony-stimulating factors (G-CSF and GM-CSF), no significant differences were observed among the groups (Suppl. Figure 3D). Chemokines exhibited distinct patterns of variation between the inflammation-induced group and the iMSC-treated group. iMSCs significantly reduced RANTES and MIP-1 $\alpha$  levels (Fig. 4D) but had no significant effect on



IL-8 and Eotaxin secretion (Suppl. Figure 3E). Regarding MCP-1 (Fig. 4D), although the iMSCs+LPS+IFN- $\gamma$  group showed significantly higher levels compared to the M0+LPS+IFN- $\gamma$  group, the elevated MCP-1 in the iMSCs+LPS+IFN- $\gamma$  group cannot be solely attributed to macrophage secretion, as iMSCs themselves may secrete substantial MCP-1 under LPS+IFN- $\gamma$  stimulation. Thus, it is not possible to conclude that iMSCs co-culture promotes MCP-1 secretion by macrophages under LPS+IFN- $\gamma$  stimulation.

Immune-related cytokines are involved in the survival, proliferation, and activation of T cells, B cells, NK cells, and mast cells, thereby promoting diverse immune responses. LPS+IFN- $\gamma$  stimulation significantly increased the secretion of these cytokines (Fig. 4E, Suppl. Figure 3F), while the addition of iMSCs significantly reduced the secretion of IL-2, IL-5, IL-9, and IL-15 by macrophages under inflammatory conditions (Fig. 4E), but had no significant effect on IL-7 (Suppl. Figure 3F). These results suggest that iMSCs can suppress macrophage-mediated promotion of immune responses, thereby reflecting their immunosuppressive potential.

Overall, under the inflammatory conditions induced by LPS+IFN- $\gamma$ , iMSCs modulate macrophage cytokine secretion by reducing pro-inflammatory cytokines (IL-17, IL-1 $\beta$ ) and immune-related cytokines (IL-2, IL-5, IL-9, IL-15), increasing anti-inflammatory cytokines (IL-10) and growth factors (VEGF), and regulating the levels of chemokines (RANTES and MIP-1 $\alpha$ ). These effects suggest that iMSCs may exert anti-inflammatory, immunoregulatory, and tissue repair-promoting functions.

#### **iMSCs inhibit macrophage M1 polarization through the NF- $\kappa$ B signaling pathway**

To elucidate the molecular mechanisms underlying the inhibition of M1 macrophage polarization by iMSCs, we performed high-throughput transcriptome sequencing and analyzed the differential gene expression profiles and potential signaling pathways among four groups: the control M0 group, the group co-cultured with iMSCs (M0+iMSCs), the LPS+IFN- $\gamma$ -stimulated group (M0+LPS+IFN- $\gamma$ ), and the LPS+IFN- $\gamma$ -stimulated group co-cultured with iMSCs (M0+LPS+IFN- $\gamma$ +iMSCs). Compared with the M0 control group, 1,760 genes were downregulated and 3,034 genes were upregulated in the M0+iMSCs group (Supplementary Fig. 1A, B). In the M0+LPS+IFN- $\gamma$  group, 1,298 genes were downregulated and 1,458 genes were upregulated relative to the M0 control group (Supplementary Fig. 1A, C). Furthermore, in the M0+LPS+IFN- $\gamma$ +iMSCs group, 2,639 genes were downregulated and 3,264 genes were upregulated

compared with the M0+LPS+IFN- $\gamma$  group (Supplementary Fig. 1A, D). To identify potential signaling pathways involved in the inhibition of M1 macrophage polarization by iMSCs, we intersected the genes upregulated in the M0+LPS+IFN- $\gamma$  group compared to the control group, the genes downregulated in the M0+iMSCs group compared to the control group, and the genes downregulated in the M0+LPS+IFN- $\gamma$ +iMSCs group compared to the M0+LPS+IFN- $\gamma$  group. A total of 121 differentially expressed genes met these criteria (Fig. 5A). GO analysis was performed to elucidate the biological implications of these differentially expressed genes [34], revealing enrichment in functions related to inflammation regulation, including cellular response to lipopolysaccharide, cytokine-mediated signaling pathways, and inflammatory responses (Fig. 5B, C). Additionally, Pathway analysis based on the KEGG database was conducted to identify key pathways associated with the differentially expressed genes [35], demonstrating significant enrichment in inflammatory pathways such as the IL-17 signaling pathway, TNF signaling pathway, and NF- $\kappa$ B signaling pathway (Fig. 5D, E). The GO-Tree diagram illustrates the network relationships of key signaling pathways identified through KEGG analysis, highlighting the central role of the NF- $\kappa$ B signaling pathway in inflammatory regulation (Fig. 5F). This suggests that iMSCs may participate in the regulation of macrophage polarization by modulating the IL-17, TNF, and NF- $\kappa$ B pathways, ultimately influencing cytokine-cytokine receptor interactions.

To validate the key signaling pathways enriched by bioinformatics analysis, we performed Western blot analysis on two of the highest-ranked pathways from Pathway analysis, NF- $\kappa$ B and PI3K-AKT. M0 macrophages, derived from PMA stimulation, exhibited high levels of P-p65 expression, as PMA is a known activator of the NF- $\kappa$ B pathway (Fig. 5G). As expected, stimulation with LPS+IFN- $\gamma$  resulted in a significant increase in the ratio of P-p65/p65 and P-AKT/AKT, indicating activation of both the NF- $\kappa$ B and PI3K-AKT pathways by inflammatory stimulation. Under inflammatory conditions, co-culture with iMSCs led to a significant reduction in the P-p65/p65 ratio, while the P-AKT/AKT levels showed no significant difference compared to the LPS+IFN- $\gamma$  group (Fig. 5G-I). This suggests that iMSCs significantly inhibit the activation of the NF- $\kappa$ B signaling pathway in macrophages within an inflammatory environment, without affecting the activation of the PI3K-AKT pathway. The use of the NF- $\kappa$ B pathway activator PMA further validated the role of NF- $\kappa$ B signaling. Flow cytometry analysis revealed that the proportion of M1 macrophages was significantly higher in the LPS+IFN- $\gamma$  group compared to the M0 control group, and iMSC intervention significantly

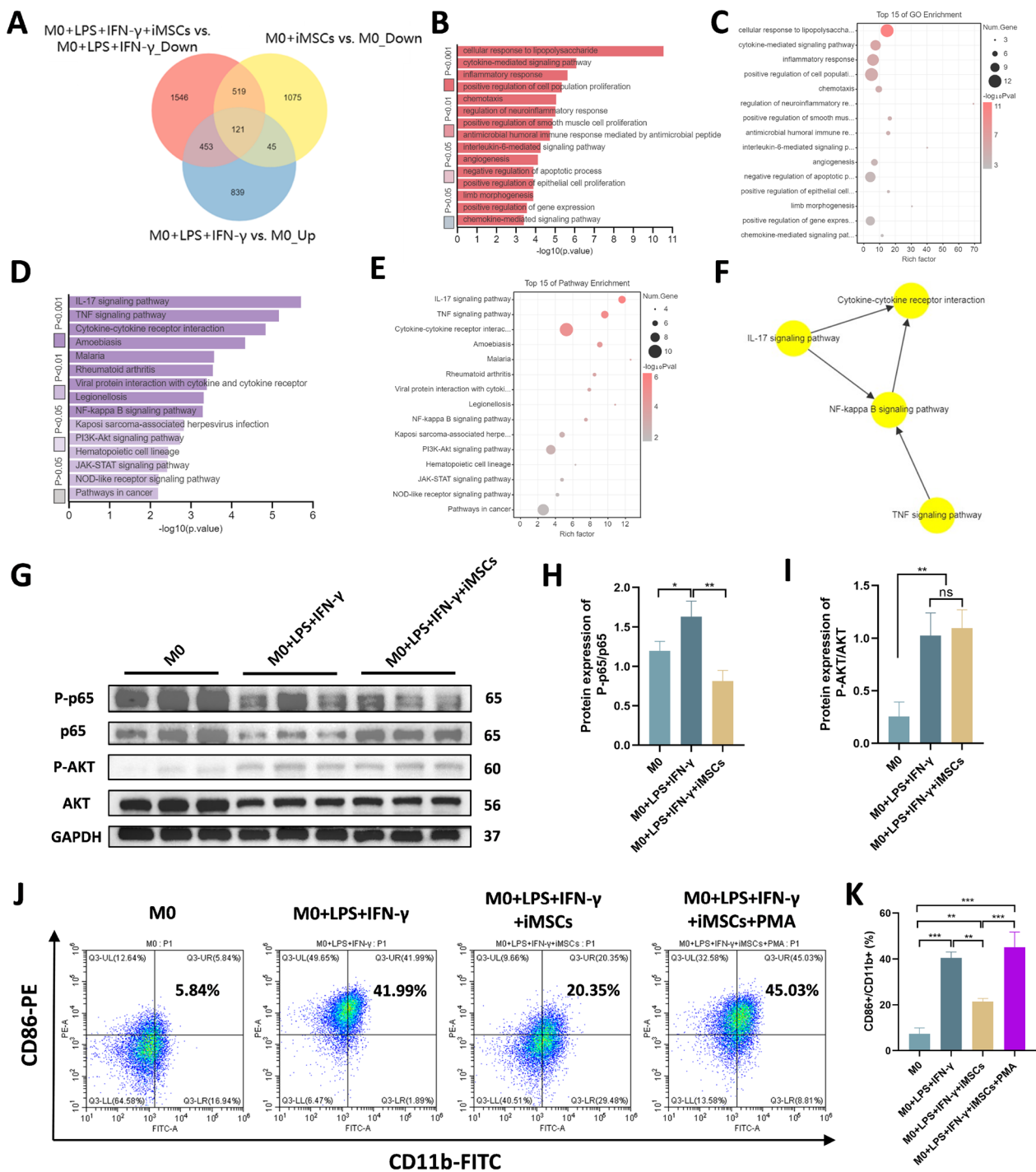


**Fig. 5** Transcriptome sequencing and pathway validation. **A** The Venn diagram illustrates the overlap of differentially expressed genes in macrophages across the different treatment groups. **B** The bar chart of GO analysis displays the functional enrichment of differentially expressed genes. **C** The bubble chart from the GO analysis provides a detailed overview of the significantly enriched gene categories. **D** The bar chart from Pathway analysis shows the enrichment of signaling pathways associated with the differentially expressed genes. **E** The bubble chart from Pathway analysis further highlights the significantly enriched signaling pathways. **F** The GO-Tree diagram illustrates the network relationships of key signaling pathways identified through KEGG analysis. **G** Western blot analysis showing the expression levels of P-p65, p65, P-AKT, and AKT proteins (Full-length blots are presented in Supplementary Fig. 2E-I). **H** Quantitative analysis of P-p65 protein expression relative to p65. **I** Quantitative analysis of P-AKT protein expression relative to AKT. **J** Flow cytometry was used to assess M1 polarization, with the upper right quadrant representing the percentage of CD11b<sup>+</sup>/CD86<sup>+</sup> M1 macrophages. **K** Flow cytometry statistical analysis indicates the differences in the proportion of CD86<sup>+</sup>/CD11b<sup>+</sup> cells among the different treatment groups. \* $P < 0.05$ , \*\* $P < 0.01$ , \*\*\* $P < 0.001$ ; ns, not significant ( $P > 0.05$ ).

reduced the proportion of M1 macrophages. Treatment with PMA reversed the anti-inflammatory effects of iMSCs, leading to an increase in the M1 macrophage proportion (Fig. J, K). These findings suggest that iMSCs exert their anti-inflammatory effects by inhibiting NF- $\kappa$ B signaling pathway, thereby suppressing M1 macrophage polarization.

#### **iMSCs modulate macrophages to preserve osteogenic potential of PDLSCs under inflammatory conditions**

PDLSCs are crucial for the repair and regeneration of periodontal tissues in periodontal disease [36, 37], and we further explored whether the modulation of macrophages by iMSCs affects the osteogenic potential of PDLSCs. The results of alkaline phosphatase (ALP) staining and ALP activity assay on day 7 demonstrated that CM from macrophages exposed to the LPS+IFN- $\gamma$ -induced inflammatory microenvironment significantly suppressed ALP activity in PDLSCs compared to CM derived from M0 macrophages. Notably, CM collected from macrophages co-cultured with iMSCs under inflammatory conditions effectively rescued ALP activity in PDLSCs (Fig. 6A, B). Similarly, the 21-day Alizarin Red staining results demonstrated that the CM from LPS+IFN- $\gamma$ -stimulated macrophages reduced mineralization deposition in PDLSCs, whereas co-culturing with iMSCs restored the mineralization ability of PDLSCs (Fig. 6C, D). The gene expression analysis exhibited a similar trend, with the CM from M0+LPS+IFN- $\gamma$  significantly inhibiting the expression of osteogenic marker genes (ALP, OCN, RUNX2, and COL-1) in PDLSCs (Fig. 6E). In contrast, the CM from M0+LPS+IFN- $\gamma$ +iMSCs reversed this effect, rescuing the expression of ALP and COL-1 at day 7 and the expression of RUNX2 and COL-1 at day 21 (Fig. 6E). These findings indicate that iMSCs protect the osteogenic capacity of PDLSCs by inhibiting M1 macrophage polarization.

#### **iMSCs injection reduces alveolar bone loss and modulates macrophage polarization in experimental periodontitis**

An experimental periodontitis mouse model was established using silk ligature, and iMSCs were injected into the buccal and palatal sides of the second maxillary molar. Micro-CT analysis (Fig. 7A) revealed significant alveolar bone resorption in the periodontitis group compared to the healthy control group, while iMSCs treatment markedly reduced alveolar bone loss. The loss of alveolar bone height (CEJ-AB distance) was significantly reduced following iMSCs injection, and both BV/TV and BMD were notably increased, demonstrating significant improvement in bone volume

parameters (Fig. 7B). The number of osteoclasts in the alveolar bone surrounding the periodontitis-affected area was significantly increased, whereas iMSCs treatment significantly reduced osteoclast activity (Fig. 7C, D). HE staining revealed marked inflammatory cell infiltration and bone tissue destruction in the periodontitis group, whereas iMSCs treatment alleviated the inflammatory response (Fig. 7E).

To further validate the therapeutic effects of iMSCs in treating periodontitis and their role in regulating macrophage polarization signaling pathways in vivo, immunohistochemistry and immunofluorescence staining were performed on periodontal tissues. Compared to the healthy group, mice in the periodontitis group exhibited a significant increase in macrophages (CD68+) and M1 macrophages (iNOS+), whereas these populations were significantly reduced in the iMSCs local injection group (Fig. 8A, B). Regarding M2 macrophages (CD206+), their expression was increased in the iMSCs treatment group compared to the periodontitis group (Fig. 8A, B); however, the proportion remained relatively low. These findings suggest that inhibition of M1 macrophage polarization may play a more critical role in the therapeutic effects of iMSCs in experimental periodontitis. Inflammatory stimuli such as LPS trigger the release and nuclear translocation of NF- $\kappa$ B p65, thereby activating the NF- $\kappa$ B signaling pathway [38]. Immunofluorescence staining of p65 nuclear translocation cells was used to assess the activation of the NF- $\kappa$ B signaling pathway. In merged images, pink areas represent cells with p65 nuclear translocation, indicating activation of the NF- $\kappa$ B signaling pathway. Compared to the healthy group, the periodontitis group exhibited a significant increase in p65 nuclear-translocated cells, indicative of NF- $\kappa$ B pathway activation. Following local injection of iMSCs, p65 nuclear-translocated cells was significantly reduced (Fig. 8C, D), demonstrating that iMSCs effectively inhibited NF- $\kappa$ B signaling. In addition, consistent with the results of the in vitro multi-cytokine assay, iMSCs also suppressed the expression of the inflammatory factor IL-17 in periodontal tissues (Fig. 8E, F). Collectively, these in vivo findings further confirm the results of in vitro experiments and bioinformatics analyses, indicating that iMSCs alleviate alveolar bone loss in periodontitis by inhibiting M1 macrophage polarization, an effect that may be mediated through suppression of IL-17 and NF- $\kappa$ B signaling pathway.

#### **Discussion**

In this study, we conducted the first analysis of the regulatory effects of induced pluripotent stem cell-derived mesenchymal stem cells (iMSCs) on



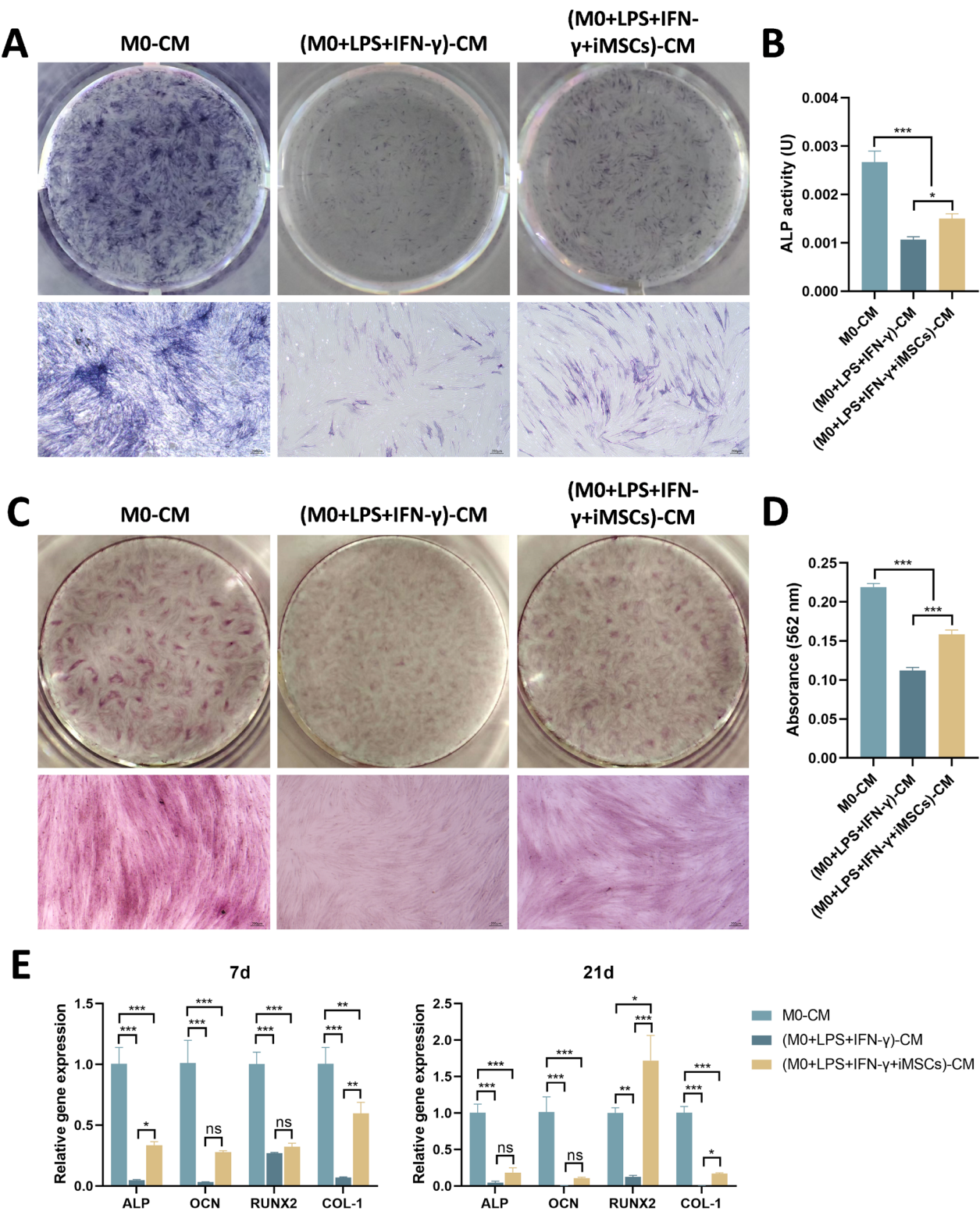


**Fig. 6** Effects of osteogenic induction medium containing conditioned medium (CM) from different macrophage groups on the osteogenic differentiation of PDLSCs. **A** ALP staining of PDLSCs on day 7. **B** Quantitative measurement of ALP activity in PDLSCs on day 7. **C** Alizarin Red staining of mineralized nodules formed by PDLSCs on day 21. **D** Semi-quantitative analysis of mineralized nodule formation in PDLSCs on day 21. **E** Relative expression levels of osteogenesis-related genes (ALP, OCN, RUNX2, and COL-1) on days 7 and 21. \* $P < 0.05$ , \*\* $P < 0.01$ , \*\*\* $P < 0.001$ ; ns, not significant ( $P > 0.05$ )



macrophage polarization and their therapeutic efficacy in a periodontitis model. Our results demonstrated that iMSCs effectively suppressed M1 macrophage polarization, alleviated inflammation-induced oxidative stress, restored the osteogenic capacity of PDLSCs under inflammatory conditions, and mitigated alveolar bone loss in mice with periodontitis. Detailed analysis of cytokines and signaling pathways revealed that iMSCs regulate macrophage polarization via the NF- $\kappa$ B signaling pathway. This study provides novel insights into the mechanisms by which iMSCs alleviate inflammation and regulate immune balance, offering a new scientific basis and potential therapeutic targets for their application in periodontitis treatment.

It is well established that MSCs possess immunomodulatory properties, and iMSCs also exhibit significant immunoregulatory potential. As a novel MSCs source, whether the immunomodulatory functions of iMSCs differ from those of traditionally derived MSCs has attracted attention. Studies have shown that iMSCs can downregulate the cytolytic activity of NK cells and exhibit greater resistance to pre-activated NK cells than adult bone marrow-derived MSCs [39]. Furthermore, iMSCs prolong the survival of hindlimbs in a vascularized composite allograft model in rats, with their regulatory effects on T cells being comparable to those of bone marrow- and adipose-derived MSCs [40]. Another study reported that iMSCs, as a unique MSCs subtype, possess greater immunosuppressive capacity against allogeneic T-cell stimulation than their donor-matched parental MSCs [20]. These findings suggest that the immunoregulatory capabilities of iMSCs are at least equivalent to, if not superior to, those of traditional MSCs sources.

Studies have reported that iMSCs exhibit immunomodulatory functions on various immune cells, including NK cells, T cells, and dendritic cells [23, 39, 41, 42]. In this study, we were the first to investigate the effects of iMSCs on macrophage polarization, providing an additional layer of understanding of the immunomodulatory capabilities of iMSCs. Previous researches have demonstrated that MSCs can exert therapeutic effects by regulating macrophage polarization. For instance, human gingiva-derived

MSCs induce M2 macrophage polarization and enhance skin wound healing [43]. Dental follicle-derived MSCs improve lipopolysaccharide-induced inflammation by promoting M2 polarization via secretion of TGF- $\beta$ 3 and TSP-1 [44]. Adipose-derived MSCs facilitate M2 polarization, suppress TGF- $\beta$ /Smad signaling, and ameliorate renal fibrosis in rats [45]. Similarly, adipose-derived MSCs inhibit NLRP3 inflammasomes, induce the production of anti-inflammatory cytokines (e.g., IL-10 and TGF- $\beta$ ), reduce NF- $\kappa$ B activity, and promote M2 polarization, thereby mitigating experimental gouty arthritis [46]. Our findings revealed that iMSCs suppress M1 macrophage polarization under inflammatory conditions, highlighting that iMSCs, like traditional MSCs sources, possess immunomodulatory capabilities to regulate macrophage polarization.

In chronic inflammatory diseases, macrophages undergo dynamic shifts between pro-inflammatory M1 and anti-inflammatory M2 macrophages [47]. Although the proportion of macrophage populations in periodontal lesions is relatively small [48], macrophages play a critical role in the progression and healing of periodontitis [4]. Severe chronic periodontitis is characterized by an imbalance in M1/M2 macrophage populations, with a predominance of M1 polarization [7]. Reducing the M1/M2 ratio and osteoclastogenesis has been shown to alleviate the pathogenicity of periodontitis [8]. As an immunomodulatory stem cell type, MSCs demonstrate promising potential in periodontitis treatment. Local injection of BMSCs effectively suppresses inflammation and significantly reduces alveolar bone resorption in rat models of experimental periodontitis [49]. Similarly, preliminary findings by Yang et al. revealed that tail vein and local injections of TSG-6-overexpressing iMSCs significantly reduced inflammation and suppressed alveolar bone resorption in experimental periodontitis models [50]. In this study, we validated the therapeutic effects of iMSCs *in vivo* in experimental periodontitis models, corroborating the findings of Yang et al., and further explored the relationship between iMSCs therapy and macrophage polarization. Comparatively, Li et al. demonstrated that adipose-derived MSCs regulate macrophage polarization via an IDO-dependent Kyn-AhR-NRF2 pathway, leading to a reduction in the local

(See figure on next page.)

**Fig. 7** Protective effects of iMSCs on alveolar bone loss in periodontitis mice. **A** Micro-CT reconstruction images show the morphological changes of the jawbone in healthy, periodontitis, and iMSCs treatment groups of mice. **B** Quantitative Micro-CT analysis, including measurements of CEJ-AB distance, BMD, and BV/TV. **C** Quantitative results of the TRAP-positive area surrounding the alveolar bone in mice. **D** TRAP staining revealing osteoclast activity around the alveolar bone in mice. Scale bars: 100  $\mu$ m (upper panels) and 50  $\mu$ m (lower panels). **E** HE staining demonstrating histological changes in periodontal tissues of the healthy, periodontitis, and iMSCs-treated groups. Scale bars: 100  $\mu$ m (upper panels) and 50  $\mu$ m (lower panels). \* $P$  < 0.05, \*\* $P$  < 0.01, \*\*\* $P$  < 0.001; ns, not significant ( $P$  > 0.05)

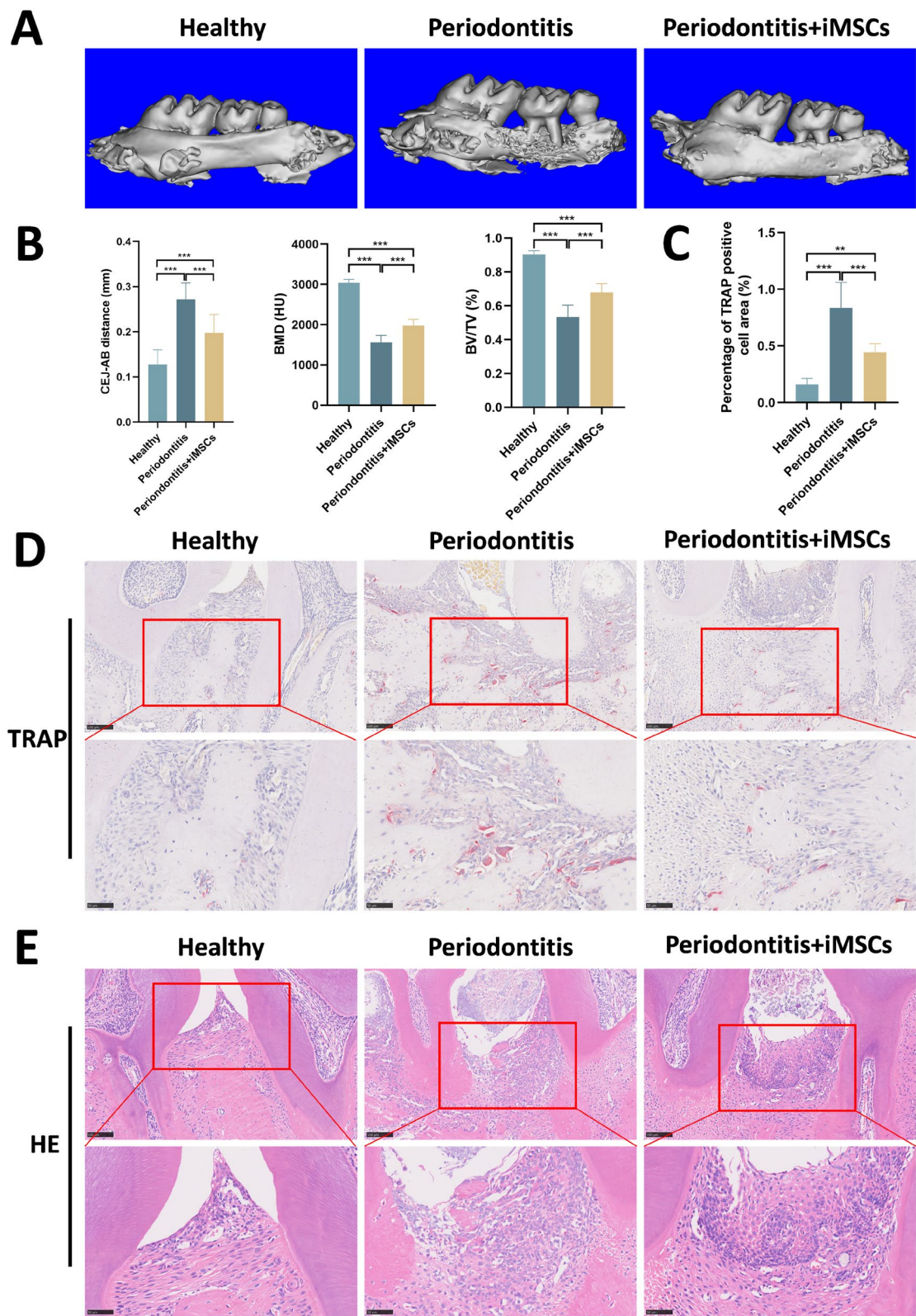


**Fig. 7** (See legend on previous page.)

M1/M2 macrophage ratio and attenuation of ligature-induced periodontitis [51]. Our findings align with those of Li et al., showing that local injection of iMSCs reduces the proportion of M1 macrophages in periodontal tissues, decreases the M1/M2 ratio, and alleviates periodontitis-associated alveolar bone loss.

This study further confirmed that the mechanism by which iMSCs inhibit M1 macrophage polarization is primarily mediated through the suppression of the NF- $\kappa$ B signaling pathway. NF- $\kappa$ B is a key transcription factor regulating inflammatory responses, activated in response to pathogen invasion, cellular damage, and other stress signals, ultimately inducing the expression of numerous inflammation-related genes to initiate and sustain inflammatory processes [52]. Drugs or inhibitors that suppress NF- $\kappa$ B signaling have been shown to exert protective and immunomodulatory effects [53, 54]. Moreover, the NF- $\kappa$ B signaling pathway plays a central regulatory role in macrophage polarization. Activation of NF- $\kappa$ B signaling promotes the polarization of macrophages toward the pro-inflammatory M1 phenotype, thereby exacerbating inflammation [55–57]. Conversely, blocking the NF- $\kappa$ B signaling pathway can suppress M1 polarization, reduce excessive production of pro-inflammatory factors, and mitigate tissue damage. For example, Huang et al. reported that knockdown of TET1 inhibited *Porphyromonas gingivalis* LPS/IFN- $\gamma$ -induced M1 macrophage polarization via the NF- $\kappa$ B pathway in THP-1 cells [58]. Similarly, resveratrol inhibited M1 macrophage polarization by suppressing NF- $\kappa$ B pathway activation, offering potential therapeutic benefits for isoproterenol-induced myocardial injury [59]. Furthermore, an innovative electrospun nanofibrous membrane promoted periodontal tissue regeneration by inhibiting PI3K/AKT and NF- $\kappa$ B signaling pathways, thereby suppressing M1 macrophage polarization [60]. Consistent with these findings, our study demonstrated that iMSCs reduce M1 macrophage polarization and the expression of pro-inflammatory cytokines by inhibiting NF- $\kappa$ B pathway activation, ultimately alleviating periodontal bone loss.

Oxidative stress also plays a critical role in inflammation and tissue destruction in periodontal

disease. Under inflammatory conditions, macrophage responses lead to the generation of large amounts of ROS. Excessive ROS production induces oxidative stress, activating multiple inflammation-related signaling pathways, including NF- $\kappa$ B and MAPK, which are involved in regulating macrophage polarization [61]. For example, hyperglycemia exacerbates periodontal inflammation by inducing macrophage polarization toward the M1 phenotype through excessive ROS production, whereas ROS scavengers that suppress M1 polarization can mitigate alveolar bone loss in diabetic rats with periodontitis [62]. MSC-based cell therapies have shown significant regulatory effects on oxidative stress, mitigating it through reduced ROS production and multiple mechanisms [27, 63]. Chen et al. demonstrated that adipose-derived MSCs reduced ROS levels in LPS-stimulated macrophages and alleviated oxidative stress by upregulating NRF2 and NQO1 gene and protein expression, thereby modulating macrophage polarization and reducing inflammation [51]. In this study, we found that iMSCs similarly reduced ROS release in macrophages under inflammatory conditions (LPS + IFN- $\gamma$ ) and alleviated oxidative stress by upregulating the transcription of NQO1 and CAT and increasing NQO1 protein expression. These findings align with the results of Chen et al., suggesting that NQO1 may play a critical role in mitigating macrophage oxidative stress through MSCs. This discovery provides further insights into the specific mechanisms by which iMSCs alleviate periodontal inflammation in vivo.

In the pathological environment of periodontitis, osteoblast function is significantly suppressed by inflammation [64]. Compared to PDLSCs derived from healthy periodontal ligament tissues, those derived from inflamed periodontal ligament tissues exhibit impaired function, including compromised immunomodulatory properties and markedly diminished osteogenic differentiation potential [65, 66]. Previous studies have demonstrated that conditioned medium (CM) from M1 macrophages impairs the osteogenic capacity of bone marrow-derived MSCs [67]. Similarly, we observed that the supernatant from LPS + IFN- $\gamma$ -stimulated M1 macrophages significantly inhibited the osteogenic

(See figure on next page.)

**Fig. 8** Immunofluorescence staining of macrophage markers and NF- $\kappa$ B signaling pathway in periodontal tissues. **A** Representative immunofluorescence images showing the expression of CD68, iNOS, and CD206 in periodontal tissues from Healthy, Periodontitis, and Periodontitis + iMSCs groups. **B** Quantitative analysis of the percentage of CD68+, iNOS+, and CD206+ cells among total DAPI-stained nuclei. **C** Representative immunofluorescence images of p65 in the periodontal tissues across the three groups. **D** Quantitative analysis of the number of p65 nuclear-translocated cells in each field of view. **E** Representative immunohistochemical (IHC) images of IL-17 in periodontal tissues from different experimental groups. Scale bars: 100  $\mu$ m (upper panels) and 50  $\mu$ m (lower panels). **F** Quantitative analysis of the percentage area of IL-17-positive cells per field of view. \* $P$  < 0.05, \*\* $P$  < 0.01, \*\*\* $P$  < 0.001; ns, not significant ( $P$  > 0.05)



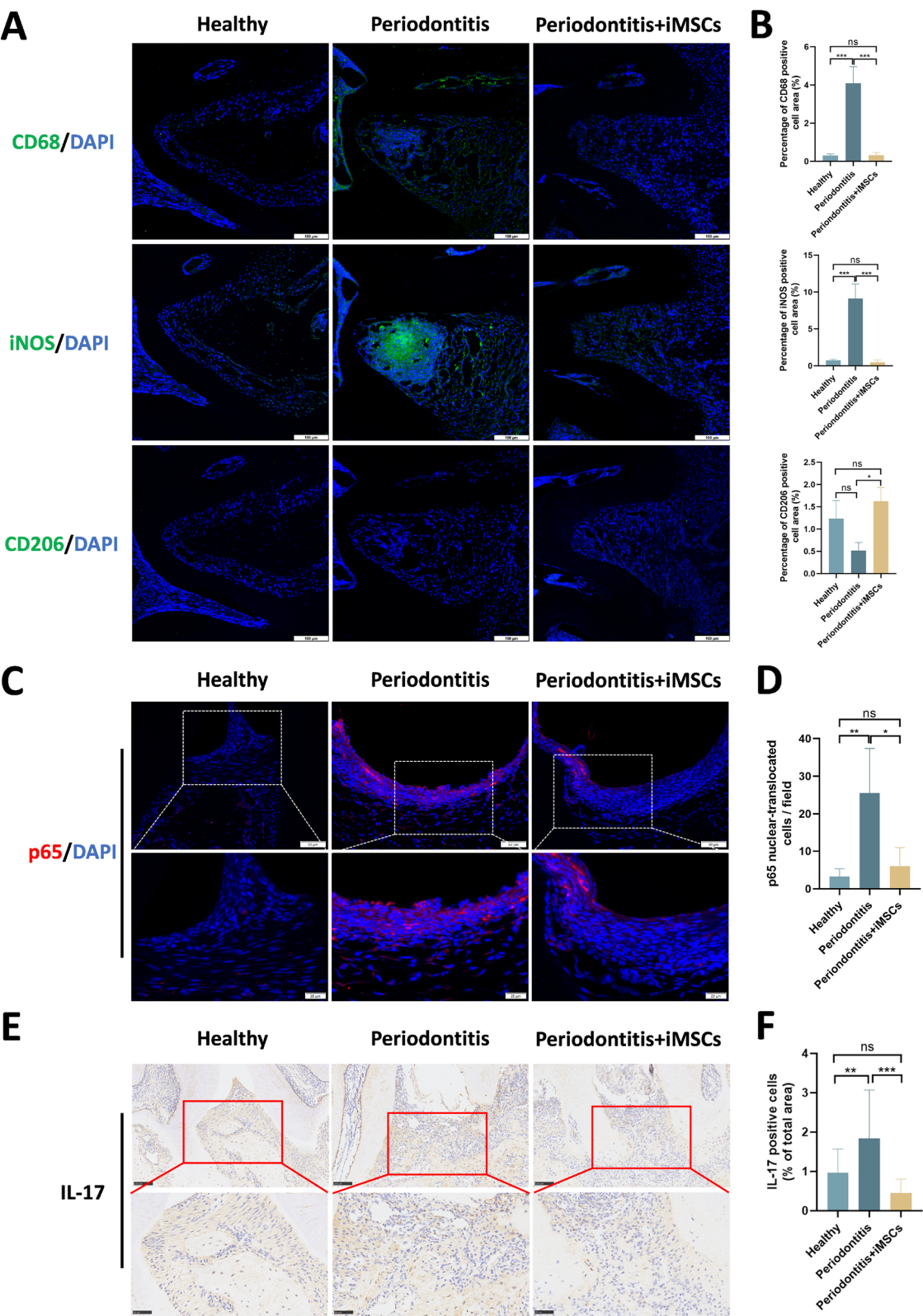


**Fig. 8** (See legend on previous page.)



ability of PDLSCs. However, when macrophages were co-cultured with iMSCs under inflammatory conditions, their supernatant partially preserved the osteogenic capacity of PDLSCs, suggesting that the immunoregulatory effects of iMSCs on macrophages play a pivotal role in restoring PDLSC function. This finding is consistent with previous research showing that adipose-derived MSCs can modulate macrophages to rescue the osteogenic potential of PDLSCs under inflammatory conditions [51]. To investigate this phenomenon further, we analyzed the cytokines secreted by macrophages, which may play a crucial role in mediating this effect. Co-culture with iMSCs reduced the levels of pro-inflammatory cytokines (IL-1 $\beta$ , IL-17) and immune-related cytokines (IL-2, IL-5, IL-9, and IL-15) while increasing anti-inflammatory factors (IL-10) and growth factors (VEGF). Additionally, iMSCs modulated the levels of chemokines (RANTES and MIP-1 $\alpha$ ). Previous studies have shown that chemokines released by immune cells recruited to the inflammatory microenvironment attract MSCs, while various inflammatory cytokines mediate the immunosuppressive response of MSCs [68]. MSCs can regulate and improve the local microenvironment in inflammatory conditions by reducing pro-inflammatory factors and increasing anti-inflammatory factors [69]. This mechanism likely explains how iMSCs alleviate inflammatory stress on PDLSCs by modulating macrophage cytokine secretion, thereby restoring the osteogenic potential of PDLSCs.

In summary, iMSCs demonstrate significant therapeutic potential in experimental periodontitis by modulating macrophage polarization. Future studies should further evaluate the long-term safety and efficacy of iMSCs to support their clinical application in periodontal diseases. Recent findings have highlighted that MSCs exert therapeutic effects through paracrine mechanisms such as extracellular vesicles [70–74] and mitochondrial transfer [75], modulating macrophage polarization and oxidative stress. In addition to the direct application of iMSCs themselves, cell-free therapies based on the paracrine effects of iMSCs hold considerable promise for the treatment of periodontitis in the future.

## Conclusions

As an emerging source of MSCs, iMSCs overcome the limitations of traditional MSCs sources in terms of availability and supply, demonstrating significant therapeutic potential in the treatment of autoimmune and inflammatory diseases. Our study revealed that iMSCs mitigate oxidative stress in macrophages under inflammatory conditions (LPS + IFN- $\gamma$ ) and inhibit

M1 macrophage polarization by regulating the NF- $\kappa$ B signaling pathway. Additionally, iMSCs modulate cytokine secretion from macrophages in inflammatory environments, reducing pro-inflammatory cytokines (IL-1 $\beta$ , IL-17) and immune-related cytokines while increasing anti-inflammatory cytokines (IL-10) and growth factors (VEGF) and modulating the levels of chemokines. Furthermore, iMSCs partially preserved the osteogenic capacity of PDLSCs under inflammatory conditions and alleviated periodontal bone loss associated with periodontitis. This study provides novel theoretical insights and potential strategies for the application of iMSCs in periodontitis treatment.

## Abbreviations

MSCs	Mesenchymal stem cells
iPSCs	Induced pluripotent stem cells
iMSCs	Induced pluripotent stem cells-derived mesenchymal stem cells
FBS	Fetal bovine serum
PMA	Phorbol 12-Myristate 13-Acetate
PDLSCs	Periodontal ligament stem cells
CM	Conditioned medium
ROS	Reactive oxygen species
RT-qPCR	Reverse transcription-quantitative polymerase chain reaction
GO analysis	Gene Ontology analysis
ALP	Alkaline phosphatase
CEJ	Cemento-enamel junction
AB	Alveolar bone crest
BMD	Bone mineral density
BV/TV	Bone volume/total volume ratio
HE staining	Hematoxylin and eosin staining
NF- $\kappa$ B	Nuclear factor kappa-light-chain-enhancer of activated B cells
IL-1 $\beta$	Interleukin-1 beta
TNF- $\alpha$	Tumor necrosis factor-alpha
IL-10	Interleukin-10
Arg-1	Arginase-1
Nrf2	Nuclear factor erythroid 2-related factor 2
iNOS	Inducible nitric oxide synthase
OCN	Osteocalcin
RUNX2	Runt-related transcription factor 2
COL-I	Collagen type I
CAT	Catalase
HO-1	Heme oxygenase-1
NQO1	NAD(P)H quinone dehydrogenase 1
LPS	Lipopolysaccharide
IFN- $\gamma$	Interferon-gamma
IHC	Immunohistochemical

## Supplementary Information

The online version contains supplementary material available at <https://doi.org/10.1186/s13287-025-04327-0>.

Supplementary material 1

## Acknowledgements

The authors declare that they have not used AI-generated work in this manuscript.

## Author contributions

LC contributed to the conception and design of the study, experimental procedures, data analysis, and manuscript writing. YQL provided technical support and data validation. CHY and PC were involved in the conception of

the study and assisted with data interpretation. YMM and YRG assisted with experimental validation. YC, YZ, and JL participated in experimental design. YL provided the iPSCs line and contributed to the conception. QXL contributed to the conception, supervised the project, and provided funding. All authors read and approved the final manuscript.

### Funding

This study was supported by the General Program of the National Natural Science Foundation of China (No. 82370956), the National Key Research and Development Program of China (No. 2023YFC2506300) and the National Nature Science Foundation of China (No. 82401105, No. 32371533).

### Availability of data and materials

All data generated or analyzed during this study are included in this published article and its supplementary information files. The transcriptomics data has been deposited in Gene Expression Omnibus database with accession number GSE283726.

### Declarations

#### Ethics approval and consent to participate

Our iPSCs are derived from peripheral blood from one female healthy donor whose written consent was obtained in accordance with the guidelines of the Peking University Health Science Center Ethical Committee. The EallBio has confirmed that there was initial ethical approval for collection of human cells, and that the donors had signed informed consent. The animal experimental protocol was approved by the Biomedical Ethics Committee of Peking University (Title: Construction of Universal Non-immunogenic iPSC-MSCs and Evaluation of Their Effects on Periodontal Tissue Regeneration; Approval No.: PUIRB-LA2023075; Date: March 1, 2023). The work has been reported in line with the ARRIVE guidelines 2.0.

#### Consent for publication

Not applicable.

#### Competing interests

The authors declare that they have no competing interests.

#### Author details

<sup>1</sup>Department of Periodontology, Peking University School and Hospital of Stomatology & National Center for Stomatology & National Clinical Research Center for Oral Diseases & National Engineering Laboratory for Digital and Material Technology of Stomatology, No. 22, Zhongguancun South Avenue, Haidian District, Beijing 100081, People's Republic of China. <sup>2</sup>First Clinical Division, Peking University School and Hospital of Stomatology & National Center for Stomatology & National Clinical Research Center for Oral Diseases & National Engineering Laboratory for Digital and Material Technology of Stomatology, No. 22, Zhongguancun South Avenue, Haidian District, Beijing 100081, People's Republic of China. <sup>3</sup>Department of Cell Biology, School of Basic Medical Sciences, Peking University Stem Cell Research Center, Peking University, Beijing, People's Republic of China.

Received: 6 December 2024 Accepted: 9 April 2025

Published online: 02 May 2025

### References

- Papapanou PN, Sanz M, Buduneli N, Dietrich T, Feres M, Fine DH, et al. Periodontitis: Consensus report of workgroup 2 of the 2017 World Workshop on the Classification of Periodontal and Peri-Implant Diseases and Conditions. *J Periodontol*. 2018;89(Suppl 1):S173–82.
- Kinane DF, Stathopoulou PG, Papapanou PN. Periodontal diseases. *Nat Rev Dis Primers*. 2017;3(1):17038.
- Sima C, Viniegra A, Glogauer M. Macrophage immunomodulation in chronic osteolytic diseases—the case of periodontitis. *J Leukoc Biol*. 2019;105(3):473–87.
- Sun X, Gao J, Meng X, Lu X, Zhang L, Chen R. Polarized macrophages in periodontitis: characteristics, function, and molecular signaling. *Front Immunol*. 2021;12: 763334.
- Yunna C, Mengru H, Lei W, Weidong C. Macrophage M1/M2 polarization. *Eur J Pharmacol*. 2020;877: 173090.
- Almubarak A, Tanagala KKK, Papapanou PN, Lalla E, Momen-Heravi F. Disruption of monocyte and macrophage homeostasis in periodontitis. *Front Immunol*. 2020;11:330.
- Zhang W, Guan N, Zhang X, Liu Y, Gao X, Wang L. Study on the imbalance of M1/M2 macrophage polarization in severe chronic periodontitis. *Technol Health Care*. 2023;31(1):117–24.
- Guo X, Huang Z, Ge Q, Yang L, Liang D, Huang Y, et al. Glipizide alleviates periodontitis pathogenicity via inhibition of angiogenesis, osteoclastogenesis and M1/M2 macrophage ratio in periodontal tissue. *Inflammation*. 2023;46(5):1917–31.
- Peng S, Fu H, Li R, Li H, Wang S, Li B, et al. A new direction in periodontitis treatment: biomaterial-mediated macrophage immunotherapy. *J Nanobiotechnology*. 2024;22(1):359.
- Shan Y, Zhang M, Tao E, Wang J, Wei N, Lu Y, et al. Pharmacokinetic characteristics of mesenchymal stem cells in translational challenges. *Signal Transduct Target Ther*. 2024;9(1):242.
- Zhou T, Yuan Z, Weng J, Pei D, Du X, He C, et al. Challenges and advances in clinical applications of mesenchymal stromal cells. *J Hematol Oncol*. 2021;14(1):24.
- Huang F, Thokerunga E, He F, Zhu X, Wang Z, Tu J. Research progress of the application of mesenchymal stem cells in chronic inflammatory systemic diseases. *Stem Cell Res Ther*. 2022;13(1):1.
- Liu C, Xiao K, Xie L. Advances in the Regulation of Macrophage Polarization by Mesenchymal Stem Cells and Implications for ALI/ARDS Treatment. *Front Immunol*. 2022;13: 928134.
- Chen Y, Yang L, Li X. Advances in Mesenchymal stem cells regulating macrophage polarization and treatment of sepsis-induced liver injury. *Front Immunol*. 2023;14:1238972.
- Takahashi K, Yamanaka S. Induction of pluripotent stem cells from mouse embryonic and adult fibroblast cultures by defined factors. *Cell*. 2006;126(4):663–76.
- Zhou M, Xi J, Cheng Y, Sun D, Shu P, Chi S, et al. Reprogrammed mesenchymal stem cells derived from iPSCs promote bone repair in steroid-associated osteonecrosis of the femoral head. *Stem Cell Res Ther*. 2021;12(1):175.
- Sabapathy V, Kumar S. hiPSC-derived iMSCs: NextGen MSCs as an advanced therapeutically active cell resource for regenerative medicine. *J Cell Mol Med*. 2016;20(8):1571–88.
- Bloor AJC, Patel A, Griffin JE, Gilleece MH, Radia R, Yeung DT, et al. Production, safety and efficacy of iPSC-derived mesenchymal stromal cells in acute steroid-resistant graft versus host disease: a phase I, multicenter, open-label, dose-escalation study. *Nat Med*. 2020;26(11):1720–5.
- Kelly K, Bloor AJC, Griffin JE, Radia R, Yeung DT, Rasko JEJ. Two-year safety outcomes of iPS cell-derived mesenchymal stromal cells in acute steroid-resistant graft-versus-host disease. *Nat Med*. 2024;30(6):1556–8.
- Lee HR, Kim S, Shin S, Jeong SY, Lee DW, Lim SU, et al. iPSC-derived MSCs are a distinct entity of MSCs with higher therapeutic potential than their donor-matched parental MSCs. *Int J Mol Sci*. 2023;24(1):881.
- Sfougataki I, Varela I, Stefanaki K, Karagiannidou A, Roubelakis MG, Kalodimos V, et al. Proliferative and chondrogenic potential of mesenchymal stromal cells from pluripotent and bone marrow cells. *Histol Histopathol*. 2020;35(12):1415–26.
- Meng F, Zhang S, Xie J, Zhou Y, Wu Q, Lu B, et al. Leveraging CD16 fusion receptors to remodel the immune response for enhancing anti-tumor immunotherapy in iPSC-derived NK cells. *J Hematol Oncol*. 2023;16(1):62.
- Gao WX, Sun YQ, Shi J, Li CL, Fang SB, Wang D, et al. Effects of mesenchymal stem cells from human induced pluripotent stem cells on differentiation, maturation, and function of dendritic cells. *Stem Cell Res Ther*. 2017;8(1):48.
- Dominici M, Le Blanc K, Mueller I, Slaper-Cortenbach I, Marini F, Krause D, et al. Minimal criteria for defining multipotent mesenchymal stromal cells. The International Society for Cellular Therapy position statement. *Cytotherapy*. 2006;8(4):315–7.
- Love MI, Huber W, Anders S. Moderated estimation of fold change and dispersion for RNA-seq data with DESeq2. *Genome Biol*. 2014;15(12):550.

26. Benjamini Y, Drai D, Elmer G, Kafkafi N, Golani I. Controlling the false discovery rate in behavior genetics research. *Behav Brain Res*. 2001;125(1–2):279–84.
27. Arakawa M, Sakamoto Y, Miyagawa Y, Nito C, Takahashi S, Nitahara-Kasahara Y, et al. iPSC-derived mesenchymal stem cells attenuate cerebral ischemia-reperfusion injury by inhibiting inflammatory signaling and oxidative stress. *Mol Ther Methods Clin Dev*. 2023;30:333–49.
28. Preethi S, Arthiga K, Patil AB, Spandana A, Jain V. Review on NAD(P) H dehydrogenase quinone 1 (NQO1) pathway. *Mol Biol Rep*. 2022;49(9):8907–24.
29. Lamb NJ, Quinlan GJ, Mumby S, Evans TW, Gutteridge JMC. Haem oxygenase shows pro-oxidant activity in microsomal and cellular systems: Implications for the release of low-molecular-mass iron. *Biochemical Journal*. 1999;344(1):153–8.
30. Chiang SK, Chen SE, Chang LC. The Role of HO-1 and Its Crosstalk with Oxidative Stress in Cancer Cell Survival. *Cells*. 2021;10(9):2401.
31. Bansal S, Biswas G, Avadhani NG. Mitochondria-targeted heme oxygenase-1 induces oxidative stress and mitochondrial dysfunction in macrophages, kidney fibroblasts and in chronic alcohol hepatotoxicity. *Redox Biol*. 2014;2:273–83.
32. Chang LC, Chiang SK, Chen SE, Yu YL, Chou RH, Chang WC. Heme oxygenase-1 mediates BAY 11–7085 induced ferroptosis. *Cancer Lett*. 2018;416:124–37.
33. Ouyang W, Rutz S, Crellin NK, Valdez PA, Hymowitz SG. Regulation and functions of the IL-10 family of cytokines in inflammation and disease. *Annu Rev Immunol*. 2011;29:71–109.
34. Ashburner M, Ball CA, Blake JA, Botstein D, Butler H, Cherry JM, et al. Gene ontology: tool for the unification of biology. *Gene Ontol Consort Nat Genet*. 2000;25(1):25–9.
35. Draghici S, Khatri P, Tarca AL, Amin K, Done A, Voichita C, et al. A systems biology approach for pathway level analysis. *Genome Res*. 2007;17(10):1537–45.
36. Seo BM, Miura M, Gronthos S, Bartold PM, Batouli S, Brahmi J, et al. Investigation of multipotent postnatal stem cells from human periodontal ligament. *Lancet (London, England)*. 2004;364(9429):149–55.
37. Liu J, Chen B, Bao J, Zhang Y, Lei L, Yan F. Macrophage polarization in periodontal ligament stem cells enhanced periodontal regeneration. *Stem Cell Res Ther*. 2019;10(1):320.
38. Lawrence T. The nuclear factor NF- $\kappa$ B pathway in inflammation. *Cold Spring Harb Perspect Biol*. 2009;1(6):a001651.
39. Giuliani M, Oudrhiri N, Noman ZM, Vernochet A, Chouaib S, Azzarone B, et al. Human mesenchymal stem cells derived from induced pluripotent stem cells down-regulate NK-cell cytolytic machinery. *Blood*. 2011;118(12):3254–62.
40. Mitsuizawa S, Ikeguchi R, Aoyama T, Ando M, Takeuchi H, Yurie H, et al. Induced pluripotent stem cell-derived mesenchymal stem cells prolong hind limb survival in a rat vascularized composite allotransplantation model. *Microsurgery*. 2019;39(8):737–47.
41. Roux C, Saviane G, Pini J, Belaid N, Dhib G, Voha C, et al. Immunosuppressive Mesenchymal Stromal Cells Derived from Human-Induced Pluripotent Stem Cells Induce Human Regulatory T Cells In Vitro and In Vivo. *Front Immunol*. 2017;8:1991.
42. Fu QL, Chow YY, Sun SJ, Zeng QX, Li HB, Shi JB, et al. Mesenchymal stem cells derived from human induced pluripotent stem cells modulate T-cell phenotypes in allergic rhinitis. *Allergy*. 2012;67(10):1215–22.
43. Zhang QZ, Su WR, Shi SH, Wilder-Smith P, Xiang AP, Wong A, et al. Human gingiva-derived mesenchymal stem cells elicit polarization of m2 macrophages and enhance cutaneous wound healing. *Stem cells (Dayton, Ohio)*. 2010;28(10):1856–68.
44. Chen X, Yang B, Tian J, Hong H, Du Y, Li K, et al. Dental Follicle Stem Cells Ameliorate Lipopolysaccharide-Induced Inflammation by Secreting TGF- $\beta$ 3 and TSP-1 to Elicit Macrophage M2 Polarization. *Cell Physiol Biochem*. 2018;51(5):2290–308.
45. Ishiuchi N, Nakashima A, Maeda S, Miura Y, Miyasako K, Sasaki K, et al. Comparison of therapeutic effects of mesenchymal stem cells derived from superficial and deep subcutaneous adipose tissues. *Stem Cell Res Ther*. 2023;14(1):121.
46. Medina JP, Bermejo-Álvarez I, Pérez-Baos S, Yáñez R, Fernández-García M, García-Olmo D, et al. MSC therapy ameliorates experimental gouty arthritis hinting an early COX-2 induction. *Front Immunol*. 2023;14:1193179.
47. Tardito S, Martinelli G, Soldano S, Paolino S, Pacini G, Patane M, et al. Macrophage M1/M2 polarization and rheumatoid arthritis: A systematic review. *Autoimmun Rev*. 2019;18(11): 102397.
48. Thorbert-Mros S, Larsson L, Berglundh T. Cellular composition of long-standing gingivitis and periodontitis lesions. *J Periodontol Res*. 2015;50(4):535–43.
49. Lu L, Liu Y, Zhang X, Lin J. The therapeutic role of bone marrow stem cell local injection in rat experimental periodontitis. *J Oral Rehabil*. 2020;47(Suppl 1):73–82.
50. Yang H, Apreio RM, Zhou X, Wang Q, Zhang W, Ding Y, et al. Therapeutic effect of TSG-6 engineered iPSC-derived MSCs on experimental periodontitis in rats: a pilot study. *PLoS ONE*. 2014;9(6): e100285.
51. Li H, Yuan Y, Chen H, Dai H, Li J. Indoleamine 2,3-dioxygenase mediates the therapeutic effects of adipose-derived stromal/stem cells in experimental periodontitis by modulating macrophages through the kynurenine-AhR-NRF2 pathway. *Mol Metab*. 2022;66: 101617.
52. Yu H, Lin L, Zhang Z, Zhang H, Hu H. Targeting NF- $\kappa$ B pathway for the therapy of diseases: mechanism and clinical study. *Signal Transduct Target Ther*. 2020;5(1):209.
53. Pei C, Zhang Y, Wang P, Zhang B, Fang L, Liu B, et al. Berberine alleviates oxidized low-density lipoprotein-induced macrophage activation by downregulating galectin-3 via the NF- $\kappa$ B and AMPK signaling pathways. *Phytother Res*. 2019;33(2):294–308.
54. Wang S, Lu M, Wang W, Yu S, Yu R, Cai C, et al. Macrophage Polarization Modulated by NF- $\kappa$ B in Polylactide Membranes-Treated Peritendinous Adhesion. *Small*. 2022;18(13): e2104112.
55. Wu X, Wang Z, Shi J, Yu X, Li C, Liu J, et al. Macrophage polarization toward M1 phenotype through NF- $\kappa$ B signaling in patients with Behçet's disease. *Arthritis Res Ther*. 2022;24(1):249.
56. He X, Wang B, Deng W, Cao J, Tan Z, Li X, et al. Impaired bisecting GlcNAc reprogrammed M1 polarization of macrophage. *Cell Commun Signal*. 2024;22(1):73.
57. Zhu X, Sun Y, Yu Q, Wang X, Wang Y, Zhao Y. Exosomal lncRNA GAS5 promotes M1 macrophage polarization in allergic rhinitis via restraining mTORC1/ULK1/ATG13-mediated autophagy and subsequently activating NF- $\kappa$ B signaling. *Int Immunopharmacol*. 2023;121: 110450.
58. Huang Y, Tian C, Li Q, Xu Q. TET1 Knockdown Inhibits *Porphyromonas gingivalis* LPS/IFN- $\gamma$ -Induced M1 Macrophage Polarization through the NF- $\kappa$ B Pathway in THP-1 Cells. *Int J Mol Sci*. 2019;20(8):2023.
59. Li Y, Feng L, Li G, An J, Zhang S, Li J, et al. Resveratrol prevents ISO-induced myocardial remodeling associated with regulating polarization of macrophages through VEGF-B/AMPK/NF- $\kappa$ B pathway. *Int Immunopharmacol*. 2020;84: 106508.
60. Han X, Wang F, Ma Y, Lv X, Zhang K, Wang Y, et al. TPG-functionalized PLGA/PCL nanofiber membrane facilitates periodontal tissue regeneration by modulating macrophages polarization via suppressing PI3K/AKT and NF- $\kappa$ B signaling pathways. *Mater Today Bio*. 2024;26: 101036.
61. Rendra E, Riabov V, Mossel DM, Sevastyanova T, Harmsen MC, Kzhyskowska J. Reactive oxygen species (ROS) in macrophage activation and function in diabetes. *Immunobiology*. 2019;224(2):242–53.
62. Zhang B, Yang Y, Yi J, Zhao Z, Ye R. Hyperglycemia modulates M1/M2 macrophage polarization via reactive oxygen species overproduction in ligature-induced periodontitis. *J Periodontol Res*. 2021;56(5):991–1005.
63. Feng B, Feng X, Yu Y, Xu H, Ye Q, Hu R, et al. Mesenchymal stem cells shift the pro-inflammatory phenotype of neutrophils to ameliorate acute lung injury. *Stem Cell Res Ther*. 2023;14(1):197.
64. Graves DT, Li J, Cochran DL. Inflammation and uncoupling as mechanisms of periodontal bone loss. *J Dent Res*. 2011;90(2):143–53.
65. Tang HN, Xia Y, Yu Y, Wu RX, Gao LN, Chen FM. Stem cells derived from “inflamed” and healthy periodontal ligament tissues and their sheet functionalities: a patient-matched comparison. *J Clin Periodontol*. 2016;43(1):72–84.
66. Lei F, Li M, Lin T, Zhou H, Wang F, Su X. Treatment of inflammatory bone loss in periodontitis by stem cell-derived exosomes. *Acta Biomater*. 2022;141:333–43.
67. He XT, Li X, Yin Y, Wu RX, Xu XY, Chen FM. The effects of conditioned media generated by polarized macrophages on the cellular behaviours of bone marrow mesenchymal stem cells. *J Cell Mol Med*. 2018;22(2):1302–15.

68. Ren G, Zhang L, Zhao X, Xu G, Zhang Y, Roberts AJ, et al. Mesenchymal stem cell-mediated immunosuppression occurs via concerted action of chemokines and nitric oxide. *Cell Stem Cell*. 2008;2(2):141–50.
69. Wang LT, Ting CH, Yen ML, Liu KJ, Sytwu HK, Wu KK, et al. Human mesenchymal stem cells (MSCs) for treatment towards immune- and inflammation-mediated diseases: review of current clinical trials. *J Biomed Sci*. 2016;23(1):76.
70. Xiao X, Xu M, Yu H, Wang L, Li X, Rak J, et al. Mesenchymal stem cell-derived small extracellular vesicles mitigate oxidative stress-induced senescence in endothelial cells via regulation of miR-146a/Src. *Signal Transduct Target Ther*. 2021;6(1):354.
71. Wang T, Jian Z, Baskys A, Yang J, Li J, Guo H, et al. MSC-derived exosomes protect against oxidative stress-induced skin injury via adaptive regulation of the NRF2 defense system. *Biomaterials*. 2020;257: 120264.
72. Fallah A, Hosseinzadeh Colagar A, Khosravi A, Saeidi M. Exosomes from SHED-MSC regulate polarization and stress oxidative indexes in THP-1 derived M1 macrophages. *Arch Biochem Biophys*. 2024;755: 109987.
73. Nakao Y, Fukuda T, Zhang Q, Sanui T, Shinjo T, Kou X, et al. Exosomes from TNF- $\alpha$ -treated human gingiva-derived MSCs enhance M2 macrophage polarization and inhibit periodontal bone loss. *Acta Biomater*. 2021;122:306–24.
74. Zhao J, Li X, Hu J, Chen F, Qiao S, Sun X, et al. Mesenchymal stromal cell-derived exosomes attenuate myocardial ischaemia-reperfusion injury through miR-182-regulated macrophage polarization. *Cardiovasc Res*. 2019;115(7):1205–16.
75. Burt R, Dey A, Aref S, Aguiar M, Akarca A, Bailey K, et al. Activated stromal cells transfer mitochondria to rescue acute lymphoblastic leukemia cells from oxidative stress. *Blood*. 2019;134(17):1415–29.

## Publisher's Note

Springer Nature remains neutral with regard to jurisdictional claims in published maps and institutional affiliations.